Rationally designed oral vaccines can set an evolutionary trap for *Salmonella* Typhimurium

Médéric Diard[1,2,*], Erik Bakkeren[1], Daniel Hoces[3], Verena Lentsch[3], Markus Arnoldini[3], Flurina Böhi[1,17], Kathrin Schumann-Moor[1,19], Jozef Adamcik[3], Luca Piccoli[4], Antonio Lanzavecchia[4], Beth M. Stadtmueller[5], Nicholas Donohue[6,18], Marjan W. van der Woude[6], Alyson Hockenberry[7,8], Patrick H. Viollier[9], Laurent Falquet[10,11], Daniel Wüthrich[12], Ferdinando Bonfiglio[13], Adrian Egli[12,13], Giorgia Zandomeneghi[14], Raffaele Mezzenga[3,15], Otto Holst[16], Beat H. Meier[14], Wolf-Dietrich Hardt[1,*], Emma Slack[1,3,*]

Affiliations;
1. Institute for Microbiology, Department of Biology, ETH Zürich, Zürich, Switzerland
2. Biozentrum, University of Basel, Basel, Switzerland
3. Institute for Food, Nutrition and Health, ETH Zurich, Zurich, Switzerland
4. Institute for Research in Biomedicine, Università della Svizzera italiana, Bellinzona, Switzerland
5. Department of Biochemistry, University of Illinois at Urbana-Champaign, Urbana, Illinois USA
6. York Biomedical Research Institute, Hull York Medical School, University of York, York, UK
7. Department of Environmental Microbiology, Eawag, Dubendorf, Switzerland
8. Department of Environmental Sciences, ETH Zürich, Switzerland
9. Microbiology and Molecular Medicine, University of Geneva, Geneva, Switzerland
10. Department of Biology, University of Fribourg, Fribourg, Switzerland
11. Swiss Institute of Bioinformatics, Fribourg, Switzerland
12. Infection Biology, Basel University Hospital, Basel, Switzerland
13. Department of Biomedicine, University of Basel, Basel, Switzerland
14.Institute for Physical Chemistry, ETH Zurich, Zurich, Switzerland
15. ETH Zurich, Department of Materials, Wolfgang-Pauli-Strasse 10, 8093 Zürich.
16. Forschungszentrum Borstel, Borstel, Germany
Current addresses:
17. Department of Molecular Mechanisms of Disease, University of Zurich, Zurich, Switzerland
18. Department of Orthopedics and Trauma, Medical University of Graz, Graz, Austria.
19. University of Zurich, Center of Dental Medicine, Oral Biotechnology & Bioengineering

*Corresponding authors

One sentence summary

By tracking vaccine-driven *Salmonella* evolution in the intestine, it is possible to rationally design oligovalent oral vaccines that generate an evolutionary trap.

Abstract

Secretory antibody responses (Immunoglobulin A, IgA) against repetitive bacterial surface glycans, such as O-antigens and capsules, can protect against intestinal pathogenic *Enterobacteriaceae*. However, efficacy of such immune responses has been limited by rapid glycan evolution and phase-variation. Here, we track IgA-driven O-antigen variation in *Salmonella* Typhimurium, and use this to assemble an oligovalent oral vaccine which sets an

evolutionary trap. IgA targeting all fitness-neutral O-antigen escape variants of *Salmonella* Typhimurium rapidly selected for mutants with very short O-antigen: a phenotype known to display major fitness costs and virulence attenuation in naive hosts. Evolutionary trap vaccination therefore represents an alternative concept in vaccine design. This approach capitalizes on the inevitable and rapid evolution of bacteria in the gut, and can combine protection of the individual with elimination of virulent enteropathogen reservoirs.

Main text

O-Antigen, the long repetitive glycan portion of lipopolysaccharide(*1*) (LPS), thickly carpets the surface of all *Salmonella enterica* subspecies *enterica* serovar Typhimurium (*S.*Tm) (**Fig. S1**) in the gut lumen. These glycans are sufficiently long and uniform to shield all non-protruding outer membrane proteins (e.g. most membrane channels(*2–4*)) from antibody binding(*5*). Protruding surface appendages, such as flagella or adhesins, do extend through the O-antigen. However, these are typically only expressed on a subset of the population(*6*, *7*) such that only a fraction of the baterial population can ever be clumped by antibodies against such antigens(*8*, *9*). High-affinity intestinal Immunoglobulin A (IgA) against O-antigen, induced by vaccination or infection(*10–12*), is therefore the dominant mechanism driving clumping by enchained growth and agglutination(*9*). As clumped bacteria are unable to approach the gut wall, this phenomenon provides protection from disease(*9*, *13*, *14*). However, oral vaccines targeting *Escherichia coli*- and *Salmonella* glycans typically generate weak protection(*15–19*). The ability of the bacteria to evolve or phase-vary their surface glycan antigens can be a major contributor to this failure (*7*, *20*, *21*).

We initially set out to investigate why vaccine-mediated protection fails in non-Typhoidal *Salmonellosis.* Animals that were vaccinated with a high-dose inactivated oral *S.*Tm vaccine (PA-*S.*Tm) and infected with wild-type *S.*Tm sporadically developed disease, involving both intestinal inflammation (quantified via fecal lipocalin 2, **Fig. 1A)** and tissue invasion (mesenteric lymph node colony forming units (CFU), **Fig. 1B**). Strikingly, disease did not correlate with IgA titres specific for the wild-type vaccination strain, i.e. occurred despite robust seroconversion (**Fig. 1C**).

As the IgA response was robust, we investigated the phenotype of *S.*Tm clones after growth in the gut lumen of infected mice. Notably in this model, protection is independent of intestinal colonization, i.e. the gut luminal *S.*Tm population size is similar in both protected and diseased mice(*9*). *S.*Tm clones re-isolated from the feces of "vaccinated but diseased" mice at day 3 post-infection showed weaker binding to vaccine-induced IgA than *S.*Tm clones re-isolated from feces of vaccinated protected mice (**Fig. 1D**). This suggested the importance of another phenomenon driven by IgA: the presence of IgA exerts a strong selection against the expression of cognate antigens on the surface of luminal *S.*Tm(*9*). Combined with the large population size and rapid growth of gut luminal pathogens(*9*), this generates ideal conditions for rapid evolution of IgA escape variants.

In order to identify changes in surface antigenicity of *S.*Tm, we phenotypically and genetically characterized the *S.*Tm clones from "vaccinated but diseased" mice. Based on our observation that protection critically depends on the O-antigen (*5*, *9*), we focused on O-antigen structure. The *S.*Tm O-antigen is a polymer of -mannose-α-(1→4)rhamnose-α-(1→3)galactose-α-(1→2) with an acetylated α-(1→3)-linked abequose at the mannose (**Fig 1E**). Wild-type *S.*Tm strains react strongly to O:12 typing antibodies (recognizing the triose backbone) and O:5 typing antisera (recognizing the acetylated abequose). Further, *S.*Tm has multiple options for rapidly generating O-antigen variants. *S.*Tm can shift from O:5 to O:4 (i.e. from an O-antigen with acetylated abequose, to one with non-O-acetylated abequose) by loss of function mutations in *oafA*, the abequose acetyl transferase. It can further shift between O:12 (wild-type) and O:12-2 (glucosylated) serotypes by methylation-dependent expression of a glucosyl transferase operon STM0557-0559 i.e. by phase variation (*22*, *23*).

This operon encodes the machinery to add glucose via an α-(1→4) linkage to the backbone galactose(*22*). It should be noted both O-acetylation and backbone-glucosylation represent major changes in the hydrophobicity or steric properties of the O-antigen repeat unit, which when extensively polymerized into full-length O-antigen will have major consequences for antibody binding(*24–26*).

We applied multiple techniques to determine the O-antigen structure of evolved *S.*Tm clones. Flow cytometry with serotyping antibodies (**Fig. 1F**), High Resolution-Magic Angle Spinning (HR-MAS) on intact bacteria (**Fig. S2A and B**) and ^{1}H-NMR (*27*) on purified lipopolysaccharide (**Fig. S2C**) confirmed the loss of abequose O-acetylation (O:5 to O:4) and gain of α-(1→4)-linked glucosylation of galactose (O:12 to O:12-2) in clones from vaccinated but diseased mice. The emergence of these variants was also observed at later stages during chronic mouse infections with attenuated *S.*Tm (**Fig. S3)**. This was dependent on the presence of Rag1 and IgA (**Fig. S3),** suggesting that IgA-dependent selective pressure for O-antigen switching can be generated both by vaccination and by immunity arising naturally during infection**.**

We then explored the underlying genetic mechanisms responsible for altered O-antigen structure in the evolved clones. We first determined the stability of the observed O-antigen phenotypes, i.e. whether we would see reversion during cultivation. *In vitro* serial passages of evolved clones over 5 days revealed that the switch from O:5 to O:4 was a stable, uniform phenotype (**Fig. 1F and S4A).** Sequencing of O:5-negative evolved clones revealed a common 7 base-pair contraction of a tandem repeat within the *oafA* open reading frame, generating a frame-shift and loss of function **(Fig. 2A and B)**. Targeted deletion of *oafA* (*S.*Tm$^{\Delta oafA}$) generated an identical phenotype to the 7 bp deletion (**Fig. 2B**). The same mutation was detected in deposited genomes of *S.* Tm isolates from swine(*28*) and is found in other O:5-negative serovars (e.g., *Salmonella enterica* Heidelberg CP031359.1 "Strain 5" (**Fig. S5A**)(*29*)). As there are only two copies of the 7 base-pair motif in the wild type ORF, the deletion of one 7 base-pair stretch is unlikely to be reversed(*30*) (**Fig. 2A, Fig. S5A**). Intriguingly, deposited sequences also indicate copy number variation in a 9bp repeat in the promoter region of *oafA* (**Fig. S5B**), suggesting a second possible site of microsatellite instability in this gene.

When next assessed the stability of O:12 to O:12-2 switching, and its underlying genetic mechanism. In contrast to O:5, the loss of O:12 was reversible during 3 rounds of serial passage and both wild-type and evolved clones generated a bimodal staining pattern, consistent with phase variation (**Fig. 1F and S4A and B**, **Supplementary movies A and B,** clones referred to henceforth as O:12^{Bimodal}). In line with known epigenetic regulation of the *gtrABC* operon expression(*22*), re-sequencing of the O:12^{Bimodal} strains revealed no consistent mutational pattern (supplementary table 3). Instead, a semi-quantitative full-genome methylation analysis supported that evolved O:12^{Bimodal} *S.*Tm clones form mixed populations based on DNA methylation. Populations of evolved clones presented a high proportion of chromosomes with a methylation pattern typical of the promoter of *gtrABC* in the ON state(*22*, *31*, *32*) and a minor population in the OFF state (**Fig. 2C**): a situation which is reversed in the ancestral strain. Targeted deletion of *gtrC* (*S.*Tm$^{\Delta gtrC}$), the serotype-specific glucosyl transferase of the *gtrABC* operon, abolished the ability of *S.*Tm to switch to an O:12-bimodal phenotype, even under strong *in vivo* selection (**Fig. S6**). Mathematical modeling of

O:12/O:12-2 population sizes for fixed switching rates (supplementary methods, **Fig. S4C-E**), and comparison of flow cytometry and a *lacZ* transcriptional fusion, suggests that *in vivo* selection of O:12-2-producing clones by IgA is sufficient to explain their relative proportion in the O:12^{Bimodal} population without needing to infer any change in the switching rate (**Fig. S4)**.

Therefore *S.*Tm clones with an altered O-antigen structure rapidly emerged in vaccinated mice. In order to quantify how strongly vaccine-induced IgA can select for O-antigen variants, we designed competition experiments using isogenic mutant pairs carrying targeted deletions in *oafA* and/or *gtrC.* This allowed us to study each O-antigen variant in isolation.

We first quantified selection for the genetic switch from an **O:5** to an **O:4** serotype. Competitions between *S.*Tm$^{\Delta oafA\ \Delta gtrC}$ (**O:4**, O:12-locked) and *S.*Tm$^{\Delta gtrC}$ (**O:5**, O:12-locked) were carried out in mice vaccinated against either *S.*Tm$^{\Delta oafA\ \Delta gtrC}$ (**O:4**) or *S.*Tm$^{\Delta gtrC}$ (**O:5**). IgA responses were strongly biased to recognition of the corresponding O:5 or O:4 *S.*Tm O-antigen and mediated a substantial selective advantage of expressing the alternative O-antigen variant (up to 1e7-fold by day 4, **Fig. 3A-C**). The magnitude of the selective advantage correlated tightly with the magnitude of the specific IgA response against the reactive strain (**Fig. 3B-C**). Deletion of *oafA* was fitness-neutral in naïve hosts during 4 days of infection (**Fig. 3A**). Specific IgA can therefore act as a strong evolutionary pressure selecting for mutations in genes encoding O-antigen-modifying enzymes.

We next quantified the selective advantage of phase-variation between **O:12** and **O:12-2** using strains with an *oafA*-mutant background (i.e. O:4-locked, to prevent uncontrolled O:5 to O:4 mutational changes). Mice were mock-vaccinated or vaccinated against *S.*Tm$^{\Delta oafA\ \Delta gtrC}$ (**O:12-locked**). Competitive infections were then carried out between *S.*Tm$^{\Delta oafA}$ (O:12-**phase-variable**) and *S.*Tm$^{\Delta oafA\ \Delta gtrC}$ (O:12-**locked**) strains. In line with published data, we observe a very mild fitness benefit of O:12 phase variation in niave mice. In contrast, phase-variation was a major benefit to *S.*Tm in a subset of vaccinated animals (**Fig. 3D**). On closer examination, we observed considerable variation in the bias of IgA towards recognition of O:12 only, or of O:12 and O:12-2 with similar titres, likely due to the stochastic nature of antibody generation towards different epitopes of the O-antigen repeat. In fact, a benefit of phase-variation (i.e. a low competitiveness of the phase-locked strain) correlated with a weak anti-O:12-2 IgA response. i.e. phase-variation is beneficial whenever the phase variant is poorly bound by IgA (**Fig. 3E**). Correspondingly, O:12-phase variation, vaccine escape and inflammation were largely observed in mice where IgA bound poorly to the O:12-2 variant (**Fig 3F and G**). The mechanistic basis of this selective advantage could be confirmed by complementation of the *gtrC* gene in trans (**Fig. S7**). It is interesting to note that *gtrABC* operons are often found in temperate phage(*20*, *23*), suggesting that the ability of *S.*Tm to quickly evade IgA mediated immunity may be further promoted by co-option of phage-encoded fitness factors (morons(*33*)).

Therefore IgA escapers, i.e. *S.*Tm mutants or phase variants only weakly recognized by vaccine-induced IgA, arise within 1-3 days of infection. Wherever IgA escapers dominated we observed full invasive and inflammatory disease (**Fig. S8**). Thus, both mutation and epigenetic switching processes shape the O-antigen structure of *Salmonella* and can increase the pathogen's fitness in the intestine of mice immune to specific serotypes. These changes can occur without any major loss of pathogen fitness in naive hosts (**Fig. 3A and D**).

From these observations we hypothesized that a vaccine combining all four possible O-antigen variants (Evolutionary trap vaccine, abbreviated as PA-*S.*Tm^{ET}; generated by mixing vaccines containing the **O:5,12** *S.*Tm$^{\Delta gtrC}$, **O:4,12** *S.*Tm$^{\Delta oafA\ \Delta gtrC}$, **O:4,12-2** *S.*Tm$^{\Delta oafA}$ p*gtrABC*, and **O:5,12-2** *S.*Tm p*gtrABC* strains) should generate enhanced disease protection by cutting off the observed O-antigen escape pathways. Although this vaccine induced a broader antibody response (**Fig. 4A**), we observed equally good protection in both vaccinated groups (**Fig. S9**). However, closer observation revealed that PA-*S.*Tm^{ET} vaccination selected for another class of O-antigen variant: mutations generating a single-repeat O-antigen(*34*). These can be identified by weak binding to typing antisera (**Fig. 4B**) and by gel electrophoresis of purified LPS (**Fig.4C**). Sequencing of evolved clones revealed a large deletion encompassing the *wzyB* gene, encoding the O-antigen polymerase(*34*) (**Fig. 4E**, **Fig. S10** also found in some "non-typable" *S.*Tm isolates from human(*34*)). This deletion is mediated by site-specific recombination between direct repeats flanking the *wzyB* locus. This deletion was detected in all tested *S.*Tm short O-antigen isolates from PA-*S.*Tm^{ET} vaccinated mice across two independent experiments. We did not observe mutations in *wbaP*(*34*) (complete loss of O-antigen) or *opvAB*(*35*) (dysregulated O-antigen length). Intestinal IgA from PA-*S.*Tm$^{\Delta oafA}$ vaccinated mice showed higher titres against the long O-antigen than the single-repeat O-antigen (**Fig. 4D**). This weaker binding to the very short O-antigen is consistent with lower O-antigen abundance or loss of avidity (**Fig. 4B, Fig. S1**).

Single infections revealed that, in comparison to isogenic wild type counterparts, *wzyB*-deficient mutants (synthetic or evolved) are significantly less efficient at colonizing the gut of streptomycin pretreated naïve mice **(Fig. 4F**), disseminating systemically (**Fig. 4G**) and triggering inflammation (**Fig. 4H**). This attenuation can be attributed to compromised outer membrane integrity(*36*) (**Fig S11**).

We then tested whether IgA-mediated selection could drive outgrowth of clean *wzyB* deletion mutants. Competitions between *S.*Tm$^{\Delta oafA\ \Delta gtrC}$ (O:4,12-locked**, long O-antigen)** and *S.*Tm$^{\Delta oafA\ \Delta gtrC\ \Delta wzyB}$ (O:4,12-locked**, single repeat O-antigen)** mutants in the intestine of vaccinated and mock-vaccinated or antibody-deficient mice revealed a large fitness cost of the *wzyB* deletion in naive animals, as observed in earlier studies(*34*, *37*) (**Fig. 4I)**. However, in the gut of vaccinated mice, the fitness cost of decreased outer-membrane integrity in *wzyB* mutants was clearly outweighed by the benefit of avoiding O-antigen specific IgA binding (**Fig. 4I**). Vaccinated IgA$^{-/-}$ mice were indistinguishable from naive mice in these experiments, i.e. IgA and not any other effect of the vaccine was responsible for the phenotype. PA-*S.*Tm^{ET}-elicited IgA can therefore select for mutants with a fitness cost in naïve hosts.

To demonstrate that vaccine-induced IgA, and not further genetic change in *S.*Tm drive this out-competition, we carried out fecal transfer experiments. Full fecal pellets from PA-S.Tm^{ET} vaccinated mice that had been infected for 4 days with the short/long O-antigen mixture were delivered to streptomycin-treated naïve hosts. *S.*Tm$^{\Delta oafA\ \Delta gtrC\ \Delta wzyB}$ (single-repeat O-antigen) dominated the population in the donor feces. However, on transfer to the naive environment the *wzyB* mutant was rapidly out-competed by the *S.*Tm$^{\Delta oafA\ \Delta gtrC}$ (full length O-antigen) (**Fig. 4J-L**). Thus, outgrowth in vaccinated mice is not due to compensatory mutations in the *wzyB* mutants, but to antibody-mediated selection. In real transmission settings, for example between farm animals where the intestinal niche is limited and transmission includes a period of exposure to environmental stresses, we expect these mutants to transmit very poorly.

In conclusion IgA induced by "Evolutionary Trap" vaccines can drive the outgrowth of *S.*Tm mutants producing very short O-antigens. Such mutants have a major fitness disadvantage on transmission into naive hosts, with important implications for disease spread. While the cocktail of O-antigen variants incorporated into evolutionary trap vaccines will be strain-specific, the relative ease of production and low costs of inactivated whole-cell oral vaccines suggest that this could be feasible either for pandemic strain targeting, personalized medicine or farm-specific vaccines.

Intestinal bacteria, which typically form large populations that evolve rapidly, have proven highly challenging to target with standard vaccine design: i.e. vaccines targeting a single conserved antigen. Here we suggest an alternative strategy, which turns the rapid evolution of gut bacteria from a major challenge into an advantage. Using oligovalent vaccines, we can generate a breadth of IgA responses against all fitness-neutral O-antigen modifications. These force the emergence of *S.*Tm variants with a fitness disadvantage in naïve hosts. The "Evolutionary trap" approach therefore has considerable potential as prophylaxis for diseases caused by common, increasingly antibiotic resistant, *Enterobacteriaceae* in both humans and farm animals.

References

1. B. Liu, Y. A. Knirel, L. Feng, A. V. Perepelov, S. N. Senchenkova, P. R. Reeves, L. Wang, Structural diversity in *Salmonella* O antigens and its genetic basis. *FEMS Microbiol. Rev.* **38**, 56–89 (2014).
2. P. van der Ley, P. de Graaff, J. Tommassen, Shielding of Escherichia coli outer membrane proteins as receptors for bacteriophages and colicins by O-antigenic chains of lipopolysaccharide. *J. Bacteriol.* **168**, 449–451 (1986).
3. P. van der Ley, O. Kuipers, J. Tommassen, B. Lugtenberg, O-antigenic chains of lipopolysaccharide prevent binding of antibody molecules to an outer membrane pore protein in Enterobacteriaceae. *Microb. Pathog.* **1**, 43–9 (1986).
4. A. T. Bentley, P. E. Klebba, Effect of lipopolysaccharide structure on reactivity of antiporin monoclonal antibodies with the bacterial cell surface. *J. Bacteriol.* **170**, 1063–8 (1988).
5. K. Moor, S. Y. Wotzka, A. Toska, M. Diard, S. Hapfelmeier, E. Slack, Peracetic Acid Treatment Generates Potent Inactivated Oral Vaccines from a Broad Range of Culturable Bacterial Species. *Front. Immunol.* **7**, 34 (2016).
6. N. E. Freed, O. K. Silander, B. Stecher, A. Böhm, W.-D. Hardt, M. Ackermann, A simple screen to identify promoters conferring high levels of phenotypic noise. *PLoS Genet.* **4**, e1000307 (2008).
7. M. W. van der Woude, A. J. Bäumler, Phase and antigenic variation in bacteria. *Clin. Microbiol. Rev.* **17**, 581–611, table of contents (2004).
8. I. D. Iankov, D. P. Petrov, I. V. Mladenov, I. H. Haralambieva, O. K. Kalev, M. S. Balabanova, I. G. Mitov, Protective efficacy of IgA monoclonal antibodies to O and H antigens in a mouse model of intranasal challenge with Salmonella enterica serotype Enteritidis. *Microbes Infect.* **6**, 901–910 (2004).
9. K. Moor, M. Diard, M. E. Sellin, B. Felmy, S. Y. Wotzka, A. Toska, E. Bakkeren, M. Arnoldini, F. Bansept, A. D. Co, T. Völler, A. Minola, B. Fernandez-Rodriguez, G. Agatic, S. Barbieri, L. Piccoli, C. Casiraghi, D. Corti, A. Lanzavecchia, R. R. Regoes, C. Loverdo, R. Stocker, D. R. Brumley, W.-D. Hardt, E. Slack, High-avidity IgA protects the intestine by enchaining growing bacteria. *Nature*. **544**, 498–502 (2017).
10. K. Endt, B. Stecher, S. Chaffron, E. Slack, N. Tchitchek, A. Benecke, L. Van Maele, J.-C. J.-C. Sirard, A. J. A. J. Mueller, M. Heikenwalder, A. J. A. J. Macpherson, R. Strugnell, C. von Mering, W.-D. W.-D. Hardt, The microbiota mediates pathogen

clearance from the gut lumen after non-typhoidal salmonella diarrhea. *PLoS Pathog.* **6**, e1001097 (2010).
11. E. Valguarnera, M. F. Feldman, in *Methods in enzymology* (2017; http://www.ncbi.nlm.nih.gov/pubmed/28935107), vol. 597, pp. 285–310.
12. E. Diago-Navarro, I. Calatayud-Baselga, D. Sun, C. Khairallah, I. Mann, A. Ulacia-Hernando, B. Sheridan, M. Shi, B. C. Fries, Antibody-Based Immunotherapy To Treat and Prevent Infection with Hypervirulent Klebsiella pneumoniae. *Clin. Vaccine Immunol.* **24** (2017), doi:10.1128/CVI.00456-16.
13. O. Pabst, New concepts in the generation and functions of IgA. *Nat. Rev. Immunol.* **12**, 821–832 (2012).
14. K. P. Gopalakrishna, B. R. Macadangdang, M. B. Rogers, J. T. Tometich, B. A. Firek, R. Baker, J. Ji, A. H. P. Burr, C. Ma, M. Good, M. J. Morowitz, T. W. Hand, Maternal IgA protects against the development of necrotizing enterocolitis in preterm infants. *Nat. Med.* (2019), doi:10.1038/s41591-019-0480-9.
15. WHO | Antimicrobial resistance: global report on surveillance 2014. *WHO* (2016).
16. T. C. Darton, C. Jones, C. J. Blohmke, C. S. Waddington, L. Zhou, A. Peters, K. Haworth, R. Sie, C. A. Green, C. A. Jeppesen, M. Moore, B. A. V Thompson, T. John, R. A. Kingsley, L.-M. Yu, M. Voysey, Z. Hindle, S. Lockhart, M. B. Sztein, G. Dougan, B. Angus, M. M. Levine, A. J. Pollard, Using a Human Challenge Model of Infection to Measure Vaccine Efficacy: A Randomised, Controlled Trial Comparing the Typhoid Vaccines M01ZH09 with Placebo and Ty21a. *PLoS Negl. Trop. Dis.* **10**, e0004926 (2016).
17. B. Nagy, P. Z. Fekete, Enterotoxigenic Escherichia coli (ETEC) in farm animals. *Vet Res*. **30**, 259–84 (1999).
18. S. Leach, A. Lundgren, N. Carlin, M. Löfstrand, A.-M. Svennerholm, Cross-reactivity and avidity of antibody responses induced in humans by the oral inactivated multivalent enterotoxigenicEscherichia coli (ETEC) vaccine ETVAX. *Vaccine*. **35**, 3966–3973 (2017).
19. B. L. Bearson, S. M. D. Bearson, B. W. Brunelle, D. O. Bayles, I. S. Lee, J. D. Kich, Salmonella DIVA vaccine reduces disease, colonization and shedding due to virulent S. Typhimurium infection in swine. *J. Med. Microbiol.* **66**, 651–661 (2017).
20. R. J. Mostowy, K. E. Holt, Diversity-Generating Machines: Genetics of Bacterial Sugar-Coating. *Trends Microbiol.* **26**, 1008–1021 (2018).
21. D. Gerlach, Y. Guo, C. De Castro, S.-H. Kim, K. Schlatterer, F.-F. Xu, C. Pereira, P. H. Seeberger, S. Ali, J. Codée, W. Sirisarn, B. Schulte, C. Wolz, J. Larsen, A. Molinaro, B. L. Lee, G. Xia, T. Stehle, A. Peschel, Methicillin-resistant Staphylococcus aureus alters cell wall glycosylation to evade immunity. *Nature*. **563**, 705–709 (2018).
22. S. E. Broadbent, M. R. Davies, M. W. van der Woude, Phase variation controls expression of Salmonella lipopolysaccharide modification genes by a DNA methylation-dependent mechanism. *Mol. Microbiol.* **77**, 337–53 (2010).
23. M. R. Davies, S. E. Broadbent, S. R. Harris, N. R. Thomson, M. W. van der Woude, Horizontally acquired glycosyltransferase operons drive salmonellae lipopolysaccharide diversity. *PLoS Genet.* **9**, e1003568 (2013).
24. B. W. Sigurskjold, E. Altman, D. R. Bundle, Sensitive titration microcalorimetric study of the binding of Salmonella O-antigenic oligosaccharides by a monoclonal antibody. *Eur. J. Biochem.* **197**, 239–246 (1991).
25. D. A. Brummell, V. P. Sharma, N. N. Anand, D. Bilous, G. Dubuc, J. Michniewicz, C. R. MacKenzie, J. Sadowska, B. W. Sigurskjold, B. Sinnott, Probing the combining site of an anti-carbohydrate antibody by saturation-mutagenesis: role of the heavy-chain CDR3 residues. *Biochemistry*. **32**, 1180–7 (1993).
26. M. Yang, R. Simon, A. D. MacKerell, Jr., Conformational Preference of Serogroup B Salmonella O Polysaccharide in Presence and Absence of the Monoclonal Antibody Se155-4. *J. Phys. Chem. B*. **121**, 3412–3423 (2017).
27. K. Ilg, G. Zandomeneghi, G. Rugarabamu, B. H. Meier, M. Aebi, HR-MAS NMR

reveals a pH-dependent LPS alteration by de-O-acetylation at abequose in the O-antigen of Salmonella enterica serovar Typhimurium. *Carbohydr. Res.* **382**, 58–64 (2013).
28. E. Hauser, E. Junker, R. Helmuth, B. Malorny, Different mutations in the oafA gene lead to loss of O5-antigen expression in Salmonella enterica serovar Typhimurium. *J. Appl. Microbiol.* **110**, 248–53 (2011).
29. Y. Nakai, A. Ito, Y. Ogawa, S. D. Aribam, M. Elsheimer-Matulova, K. Shiraiwa, S. M. B. Kisaka, H. Hikono, S. Nishikawa, M. Akiba, K. Kawahara, Y. Shimoji, M. Eguchi, Determination of O:4 antigen-antibody affinity level in O:5 antigen positive and negative variants of Salmonella enterica serovar Typhimurium. *FEMS Microbiol. Lett.* **364** (2017), doi:10.1093/femsle/fnx062.
30. M. Bichara, J. Wagner, I. B. Lambert, Mechanisms of tandem repeat instability in bacteria. *Mutat. Res. Mol. Mech. Mutagen.* **598**, 144–163 (2006).
31. L. M. Bogomolnaya, C. A. Santiviago, H.-J. Yang, A. J. Baumler, H. L. Andrews-Polymenis, "Form variation" of the O12 antigen is critical for persistence of Salmonella Typhimurium in the murine intestine. *Mol. Microbiol.* **70**, 1105–19 (2008).
32. E. Kintz, C. Heiss, I. Black, N. Donohue, N. Brown, M. R. Davies, P. Azadi, S. Baker, P. M. Kaye, M. van der Woude, Salmonella enterica Serovar Typhi Lipopolysaccharide O-Antigen Modification Impact on Serum Resistance and Antibody Recognition. *Infect. Immun.* **85** (2017), doi:10.1128/IAI.01021-16.
33. H. Brussow, C. Canchaya, W.-D. Hardt, Phages and the Evolution of Bacterial Pathogens: from Genomic Rearrangements to Lysogenic Conversion. *Microbiol. Mol. Biol. Rev.* **68**, 560–602 (2004).
34. I. Szabo, M. Grafe, N. Kemper, E. Junker, B. Malorny, Genetic basis for loss of immuno-reactive O-chain in Salmonella enterica serovar Enteritidis veterinary isolates. *Vet. Microbiol.* **204**, 165–173 (2017).
35. I. Cota, M. A. Sánchez-Romero, S. B. Hernández, M. G. Pucciarelli, F. García-Del Portillo, J. Casadesús, Epigenetic Control of Salmonella enterica O-Antigen Chain Length: A Tradeoff between Virulence and Bacteriophage Resistance. *PLoS Genet.* **11**, e1005667 (2015).
36. E. R. Rojas, G. Billings, P. D. Odermatt, G. K. Auer, L. Zhu, A. Miguel, F. Chang, D. B. Weibel, J. A. Theriot, K. C. Huang, The outer membrane is an essential load-bearing element in Gram-negative bacteria. *Nature*. **559**, 617–621 (2018).
37. G. L. Murray, S. R. Attridge, R. Morona, Altering the length of the lipopolysaccharide O antigen has an impact on the interaction of Salmonella enterica serovar Typhimurium with macrophages and complement. *J. Bacteriol.* **188**, 2735–9 (2006).
38. A. Varki, R. D. Cummings, M. Aebi, N. H. Packer, P. H. Seeberger, J. D. Esko, P. Stanley, G. Hart, A. Darvill, T. Kinoshita, J. J. Prestegard, R. L. Schnaar, H. H. Freeze, J. D. Marth, C. R. Bertozzi, M. E. Etzler, M. Frank, J. F. Vliegenthart, T. Lütteke, S. Perez, E. Bolton, P. Rudd, J. Paulson, M. Kanehisa, P. Toukach, K. F. Aoki-Kinoshita, A. Dell, H. Narimatsu, W. York, N. Taniguchi, S. Kornfeld, Symbol Nomenclature for Graphical Representations of Glycans. *Glycobiology*. **25**, 1323–1324 (2015).
39. G. R. Harriman, M. Bogue, P. Rogers, M. Finegold, S. Pacheco, A. Bradley, Y. Zhang, I. N. Mbawuike, Targeted deletion of the IgA constant region in mice leads to IgA deficiency with alterations in expression of other Ig isotypes. *J. Immunol.* **162**, 2521–9 (1999).
40. H. Gu, Y. R. Zou, K. Rajewsky, Independent control of immunoglobulin switch recombination at individual switch regions evidenced through Cre-loxP-mediated gene targeting. *Cell*. **73**, 1155–64 (1993).
41. P. Mombaerts, J. Iacomini, R. S. Johnson, K. Herrup, S. Tonegawa, V. E. Papaioannou, RAG-1-deficient mice have no mature B and T lymphocytes. *Cell*. **68**, 869–77 (1992).
42. K. A. Datsenko, B. L. Wanner, One-step inactivation of chromosomal genes in Escherichia coli K-12 using PCR products. *Proc. Natl. Acad. Sci.* **97**, 6640–6645

(2000).
43. N. L. Sternberg, R. Maurer, Bacteriophage-mediated generalized transduction in Escherichia coli and Salmonella typhimurium. *Methods Enzymol.* **204**, 18–43 (1991).
44. B. Stecher, S. Hapfelmeier, C. Muller, M. Kremer, T. Stallmach, W.-D. Hardt, Flagella and Chemotaxis Are Required for Efficient Induction of Salmonella enterica Serovar Typhimurium Colitis in Streptomycin-Pretreated Mice. *Infect. Immun.* **72**, 4138–4150 (2004).
45. A. M. Bolger, M. Lohse, B. Usadel, Trimmomatic: a flexible trimmer for Illumina sequence data. *Bioinformatics*. **30**, 2114–2120 (2014).
46. H. Li, R. Durbin, Fast and accurate short read alignment with Burrows-Wheeler transform. *Bioinformatics*. **25**, 1754–1760 (2009).
47. B. J. Walker, T. Abeel, T. Shea, M. Priest, A. Abouelliel, S. Sakthikumar, C. A. Cuomo, Q. Zeng, J. Wortman, S. K. Young, A. M. Earl, Pilon: an integrated tool for comprehensive microbial variant detection and genome assembly improvement. *PLoS One*. **9**, e112963 (2014).
48. P. Cingolani, A. Platts, L. L. Wang, M. Coon, T. Nguyen, L. Wang, S. J. Land, X. Lu, D. M. Ruden, A program for annotating and predicting the effects of single nucleotide polymorphisms, SnpEff: SNPs in the genome of Drosophila melanogaster strain w1118; iso-2; iso-3. *Fly (Austin)*. **6**, 80–92 (2012).
49. K. Moor, S. Y. Wotzka, A. Toska, M. Diard, S. Hapfelmeier, E. Slack, Peracetic Acid Treatment Generates Potent Inactivated Oral Vaccines from a Broad Range of Culturable Bacterial Species. *Front. Immunol.* **7** (2016), doi:10.3389/fimmu.2016.00034.
50. M. Barthel, S. Hapfelmeier, L. Quintanilla-Martínez, M. Kremer, M. Rohde, M. Hogardt, K. Pfeffer, H. Rüssmann, W.-D. Hardt, Pretreatment of mice with streptomycin provides a Salmonella enterica serovar Typhimurium colitis model that allows analysis of both pathogen and host. *Infect. Immun.* **71**, 2839–58 (2003).
51. K. Moor, J. Fadlallah, A. Toska, D. Sterlin, M. L. Balmer, A. J. Macpherson, G. Gorochov, M. Larsen, E. Slack, Analysis of bacterial-surface-specific antibodies in body fluids using bacterial flow cytometry. *Nat. Protoc.* **11**, 1531–1553 (2016).
52. M. Arnoldini, I. A. Vizcarra, R. Peña-Miller, N. Stocker, M. Diard, V. Vogel, R. E. Beardmore, W.-D. Hardt, M. Ackermann, Bistable expression of virulence genes in salmonella leads to the formation of an antibiotic-tolerant subpopulation. *PLoS Biol.* **12**, e1001928 (2014).
53. S. van Vliet, A. Dal Co, A. R. Winkler, S. Spriewald, B. Stecher, M. Ackermann, Spatially Correlated Gene Expression in Bacterial Groups: The Role of Lineage History, Spatial Gradients, and Cell-Cell Interactions. *Cell Syst.* **6**, 496-507.e6 (2018).
54. O. Westphal, K. Jann, Bacterial Lipopolysaccharides Extraction with Phenol-Water and Further Applications of the Procedure. *Methods Carbohydr. Chem.* **5**, 83–91 (1965).
55. T. Steffens, K. Duda, B. Lindner, F.-J. Vorhölter, H. Bednarz, K. Niehaus, O. Holst, The lipopolysaccharide of the crop pathogen Xanthomonas translucens pv. translucens: chemical characterization and determination of signaling events in plant cells. *Glycobiology*. **27**, 264–274 (2017).
56. S. Ardissone, P. Redder, G. Russo, A. Frandi, C. Fumeaux, A. Patrignani, R. Schlapbach, L. Falquet, P. H. Viollier, Cell Cycle Constraints and Environmental Control of Local DNA Hypomethylation in α-Proteobacteria. *PLoS Genet.* **12**, e1006499 (2016).
57. H. Li, A statistical framework for SNP calling, mutation discovery, association mapping and population genetical parameter estimation from sequencing data. *Bioinformatics*. **27**, 2987–93 (2011).
58. D. W. Barnett, E. K. Garrison, A. R. Quinlan, M. P. Strömberg, G. T. Marth, BamTools: a C++ API and toolkit for analyzing and managing BAM files. *Bioinformatics*. **27**, 1691–2 (2011).
59. A. R. Quinlan, I. M. Hall, BEDTools: a flexible suite of utilities for comparing

genomic features. *Bioinformatics*. **26**, 841–2 (2010).
60. P. J. Kersey, J. E. Allen, I. Armean, S. Boddu, B. J. Bolt, D. Carvalho-Silva, M. Christensen, P. Davis, L. J. Falin, C. Grabmueller, J. Humphrey, A. Kerhornou, J. Khobova, N. K. Aranganathan, N. Langridge, E. Lowy, M. D. McDowall, U. Maheswari, M. Nuhn, C. K. Ong, B. Overduin, M. Paulini, H. Pedro, E. Perry, G. Spudich, E. Tapanari, B. Walts, G. Williams, M. Tello–Ruiz, J. Stein, S. Wei, D. Ware, D. M. Bolser, K. L. Howe, E. Kulesha, D. Lawson, G. Maslen, D. M. Staines, Ensembl Genomes 2016: more genomes, more complexity. *Nucleic Acids Res.* **44**, D574–D580 (2016).
61. M. RStudio, Inc., Boston, RStudio: Integrated Development for R, (available at https://www.rstudio.com/).
62. R: A Language and Environment for Statistical Computing. R Foundation for Statistical Computing, (available at https://www.r-project.org/about.html).
63. M. I. Love, W. Huber, S. Anders, Moderated estimation of fold change and dispersion for RNA-seq data with DESeq2. *Genome Biol.* **15**, 550 (2014).
64. H. Yamashita, A. Taoka, T. Uchihashi, T. Asano, T. Ando, Y. Fukumori, Single-Molecule Imaging on Living Bacterial Cell Surface by High-Speed AFM. *J. Mol. Biol.* **422**, 300–309 (2012).
65. M. Hoffmann, T. Muruvanda, M. W. Allard, J. Korlach, R. J. Roberts, R. Timme, J. Payne, P. F. McDermott, P. Evans, J. Meng, E. W. Brown, S. Zhao, Complete Genome Sequence of a Multidrug-Resistant Salmonella enterica Serovar Typhimurium var. 5- Strain Isolated from Chicken Breast. *Genome Announc.* **1** (2013), doi:10.1128/genomeA.01068-13.
66. C. Silva, E. Calva, J. L. Puente, M. B. Zaidi, P. Vinuesa, Complete Genome Sequence of Salmonella enterica Serovar Typhimurium Strain SO2 (Sequence Type 302) Isolated from an Asymptomatic Child in Mexico. *Genome Announc.* **4** (2016), doi:10.1128/genomeA.00253-16.
67. Y. Hong, M. A. Liu, P. R. Reeves, Progress in Our Understanding of Wzx Flippase for Translocation of Bacterial Membrane Lipid-Linked Oligosaccharide. *J. Bacteriol.* **200**, e00154-17 (2018).
68. S. K. Hoiseth, B. A. D. Stocker, Aromatic-dependent Salmonella typhimurium are non-virulent and effective as live vaccines. *Nature*. **291**, 238–239 (1981).
69. S. Hapfelmeier, B. Stecher, M. Barthel, M. Kremer, A. J. Müller, M. Heikenwalder, T. Stallmach, M. Hensel, K. Pfeffer, S. Akira, W.-D. Hardt, The Salmonella Pathogenicity Island (SPI)-2 and SPI-1 Type III Secretion Systems Allow *Salmonella* Serovar *typhimurium* to Trigger Colitis via MyD88-Dependent and MyD88-Independent Mechanisms. *J. Immunol.* **174**, 1675–1685 (2005).

Acknowledgements
OH acknowledges Heiko Käßner for recording NMR spectra, Regina Engel for GLC-MS, and Katharina Jakob and Sylvia Düpow for technical support. We want to thank Magdalena Schneider, Christine Kiessling, Elisabeth Schultheiss, Rosa-Maria Vesco and Clarisse Straub for the DNA extraction, library preparations and sequencing of the bacterial isolates. MD acknowledges Delphine Cornillet for serum resistance measurements.
Funding
MD is supported by a SNF professorship (PP00PP_176954). ES acknowledges the support of the Swiss National Science Foundation (40B2-0_180953, 310030_185128) and Gebert Rüf Microbials (GR073_17). BMS acknowledges the support of R01 AI041239/AI/NIAID NIH HHS/United States. WDH acknowledges support by grants from the Swiss National Science Foundation (SNF; 310030B-173338), the Promedica Foundation, Chur and the Helmut Horten Foundation. EB is supported by a Boehringer Ingelheim Fonds PhD fellowship. BM acknowledges support by the Swiss National Science Foundation (200020_159707).
Author contributions
MD, WDH and ES designed the project and wrote the paper. MD and ES designed and carried out experiments. MvdW, BHM, RM contributed to experimental design / data interpretation. EB, DH, VL FB, KSM, AH, JA, PV, LV, DW, FB, AE, GZ, OH, MA carried out analyses shown in Fig1-4 and S1-S9. ND produced strains 891 and 931. LP, AL and BMS generated novel antibody reagents. All authors critically reviewed the manuscript.
Conflict of Interest
The authors declare that Evolutionary Trap Vaccines are covered by European patent application EP19177251.
Data and materials availability
All data and materials are in the manuscript or will be provided on request to the corresponding authors.

List of Supplementary Materials:

- Materials and Methods
- Supplementary Figures S1-11
- Supplementary Table S1-3
- Supplementary Movies 1 and 2

Figures 1-4

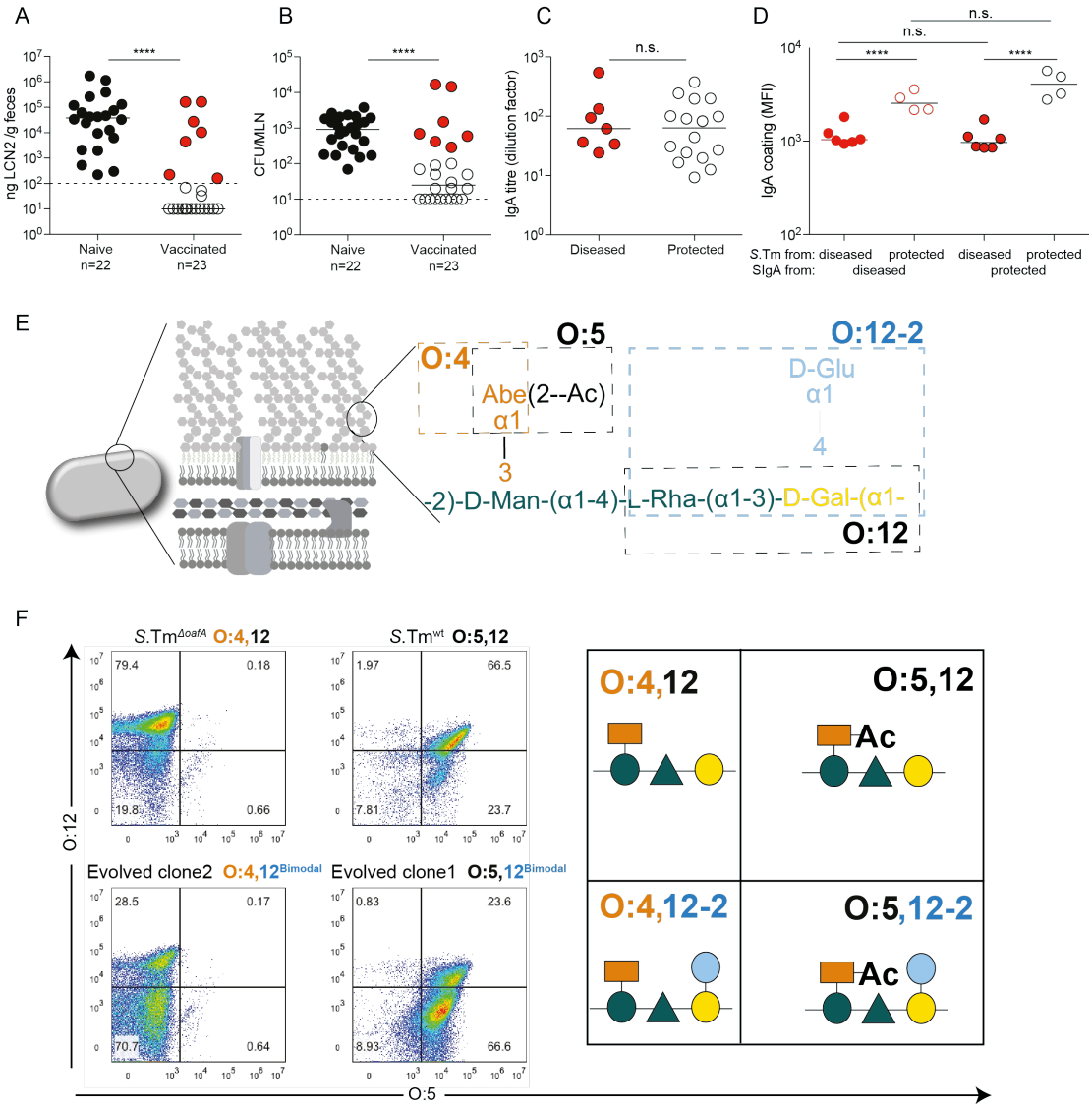

Figure 1: IgA-escape by O-antigen modification: **A-C**: Naive or PA-*S*.Tm-vaccinated (Vaccinated) mice were streptomycin-pretreated, infected (10^5 *S*.Tm^{wt} Colony forming units (CFU) per os) and analyzed 18 h later. **A**. Fecal Lipocalin 2 (LCN2) to quantify intestinal inflammation, **B**. Pathogen loads (CFU) in mesenteric lymph nodes (MLN), **C**. Intestinal IgA titres against *S*.Tm^{wt} determined by flow cytometry, for vaccinated mice with LCN2 values below (open symbols, protected) and above (filled symbols, diseased) 100ng/g. p=0.61 by Mann Whitney U test. **D**. Mice vaccinated and infected as in **A-C**. Ability of intestinal lavage IgA from diseased vaccinated mouse (red boarders) or a protected vaccinated mouse (black boarders) to recognize *S*.Tm clones re-isolated from the feces of the diseased mouse (red filled circles) or protected mouse (open circles) at day 3 post-infection. 2-way ANOVA with Bonferroni post-tests. **E**. Schematic of the O-antigen of *S*.Tm (O:5,12), and its common variants (O:4,12_2), coloured to correspond to the "Symbol Nomenclature for Glycans". **F**. Overnight cultures of the indicated *S*.Tm strains and evolved clones arising during infections with *S*.Tm^{wt} were stained with anti-O:5 and anti-O:12 antibodies, followed by fluorescent secondary reagents. Representative flow cytometry analyses of the different O-antigen types, and the "Symbol Nomenclature for Graphical Representations of Glycans"(*38*) representation of the O-antigen repeat structure present on *S*.Tm in each quadrant of the flow cytometry plots.

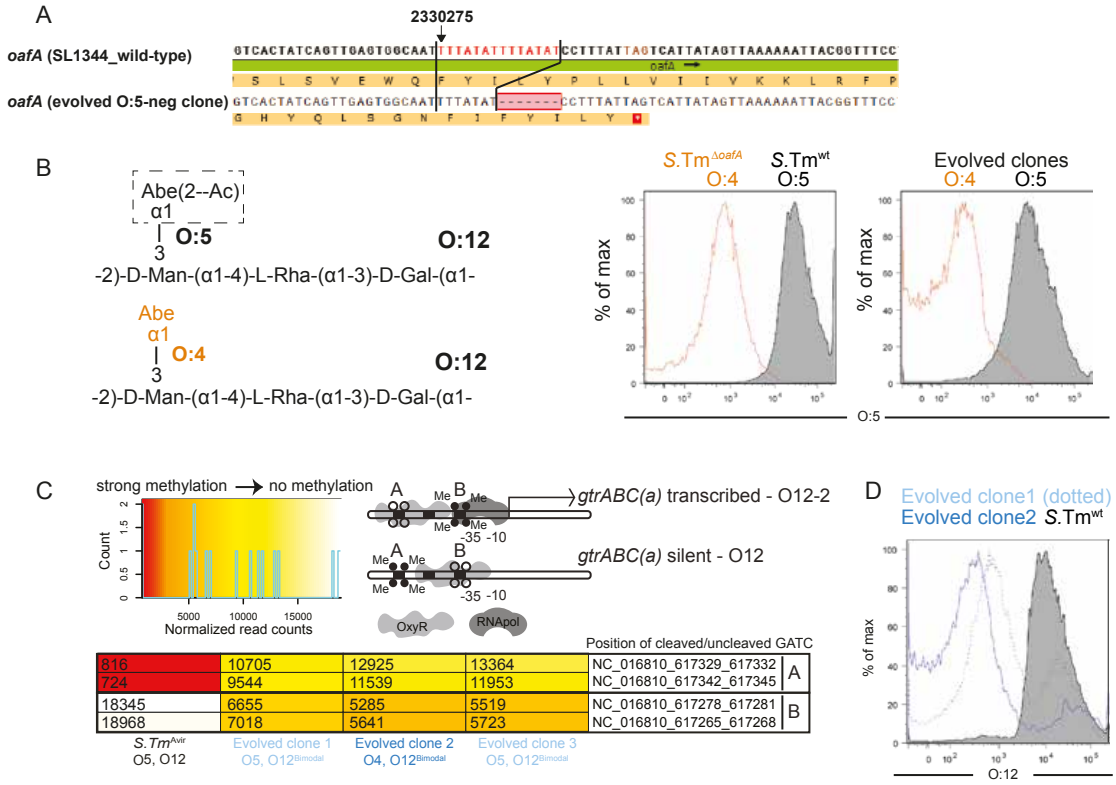

Figure 2: Genetic and epigenetic changes underlie escape: A. Alignment of the *oafA* sequence from wild type (SL1344_RS11465) and an example O:5-negative evolved clone showing the 7bp contraction (all four re-sequenced O:5-negative strains showed the same deletion). **B**. Flow cytometry staining of *S.*Tm, *S.*Tm$^{\Delta oafA}$, and two evolved clones differing in O:5 status with anti-O:5 typing sera. **C**. Methylation status of the g*trABC* promoter region in *S.*Tm, and three O:12^{Bimodal} evolved clones determined by REC-seq. Heat-scale for normalized read-counts, schematic diagram of promoter methylation associated with ON and OFF phenotypes, and normalized methylation read counts for the indicated strains **D**. Binding of an O-12-specific monoclonal antibody to *S.*Tm and O:12^{Bimodal} evolved clones, determined by bacterial flow cytometry.

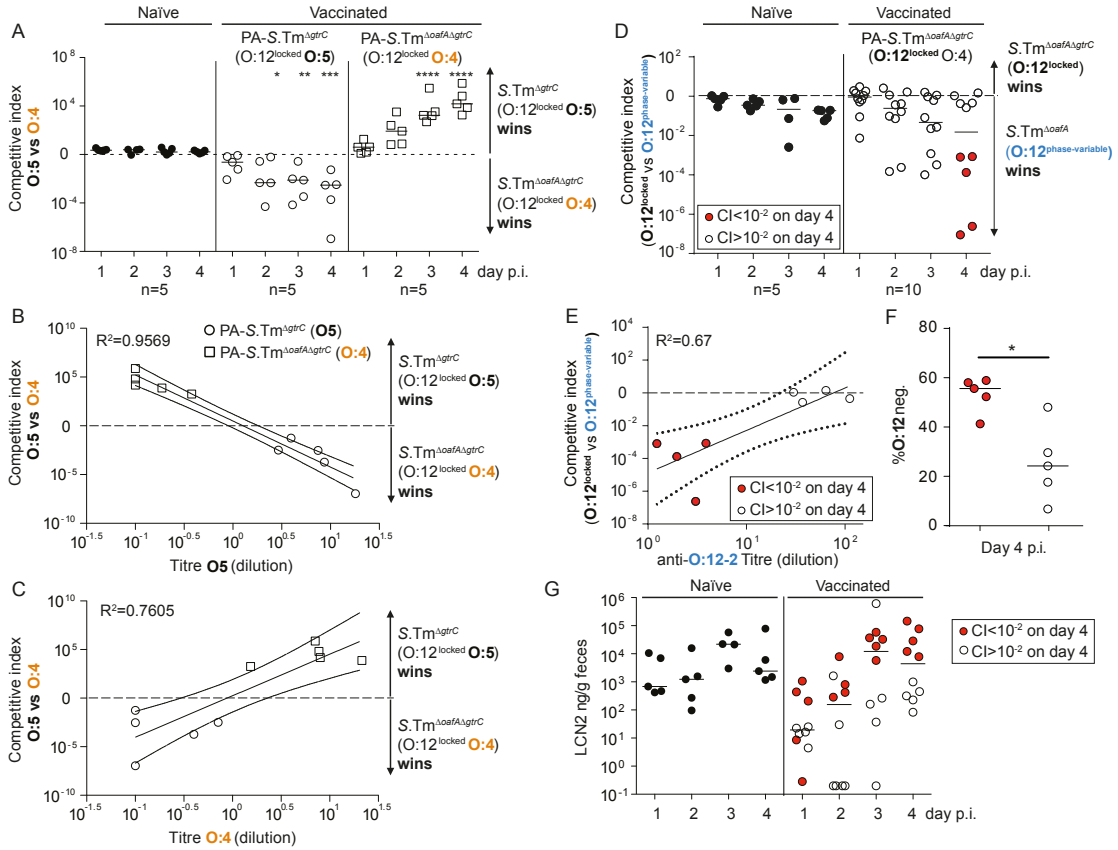

Figure 3: O-antigen modification confers a selective advantage in the presence of vaccine-induced IgA: **A-C**. Naive (closed circles), PA-*S.*Tm$^{\Delta gtrC}$-vaccinated (O:5-vaccinated, open circles) and PA-*S.*Tm$^{\Delta gtrC\Delta oafA}$-vaccinated (O:4-vaccinated, open squares) mice were streptomycin-pretreated, infected (10^5 CFU, 1:1 ratio of *S.*Tm$^{\Delta gtrC}$ and *S.*Tm$^{\Delta gtrC\ \Delta oafA}$ per os). **A**. Competitive index (CFU *S.*Tm $^{\Delta gtrC}$/CFU *S.*Tm$^{\Delta\ gtrC\ \Delta oafA}$) in feces at the indicated time-points. 2-way ANOVA with Bonferroni post-tests on log-normalized values, compared to naive mice. *p<0.05, **p<0.01,***p<0.001, ****p<0.0001. **B** and **C**. Correlation of the competitive index with the O:5-specific (**B**) and O:4-specific (**C**) intestinal IgA titre, r^2 values of the linear regression of log-normalized values. Open circles: Intestinal IgA from O:5-vaccinated mice, Open squares: Intestinal IgA from O:4-vaccinated mice. Lines indicate the best fit with 95% confidence interval **D-G.** Naive (closed circles) or PA-*S.*Tm $^{\Delta oafA\ \Delta gtrC}$-vaccinated (O:4/O:12-vaccinated, open circles and red circles) mice were streptomycin-pretreated and infected (10^5 CFU, 1:1 ratio of *S.*Tm$^{\Delta oafA}$ (O:12-2 switching) and *S.*Tm $^{\Delta oafA\ \Delta gtrC}$ (O:12-locked) per os). **D**. Competitive index (CFU *S.*Tm$^{\Delta oafA\ \Delta gtrC}$ /CFU *S.*Tm$^{\Delta oafA}$) in feces at the indicated time-points. Red circles indicate vaccinated mice with a competitive index of below 10^{-2} and are used to identify these animals in panels **D-G**. Effect of vaccination is not significant by 2-way ANOVA considering vaccination over time. **E**. Correlation of the competitive index on day 4 with the intestinal IgA titre against an O:12-2-locked *S.*Tm p*gtrABC* variant (linear regression of log-normalized values, lines indicate the best fit with 95% confidence interval). **F**. Enrichment cultures of the fecal *S.*Tm$^{\Delta oafA}$ population at day 4 were stained for O:12/O:4 and the fraction of O:12-negative *S.*Tm quantified by flow cytometry. **G**. Intestinal inflammation quantified by Fecal Lipocalin 2 (LCN2).

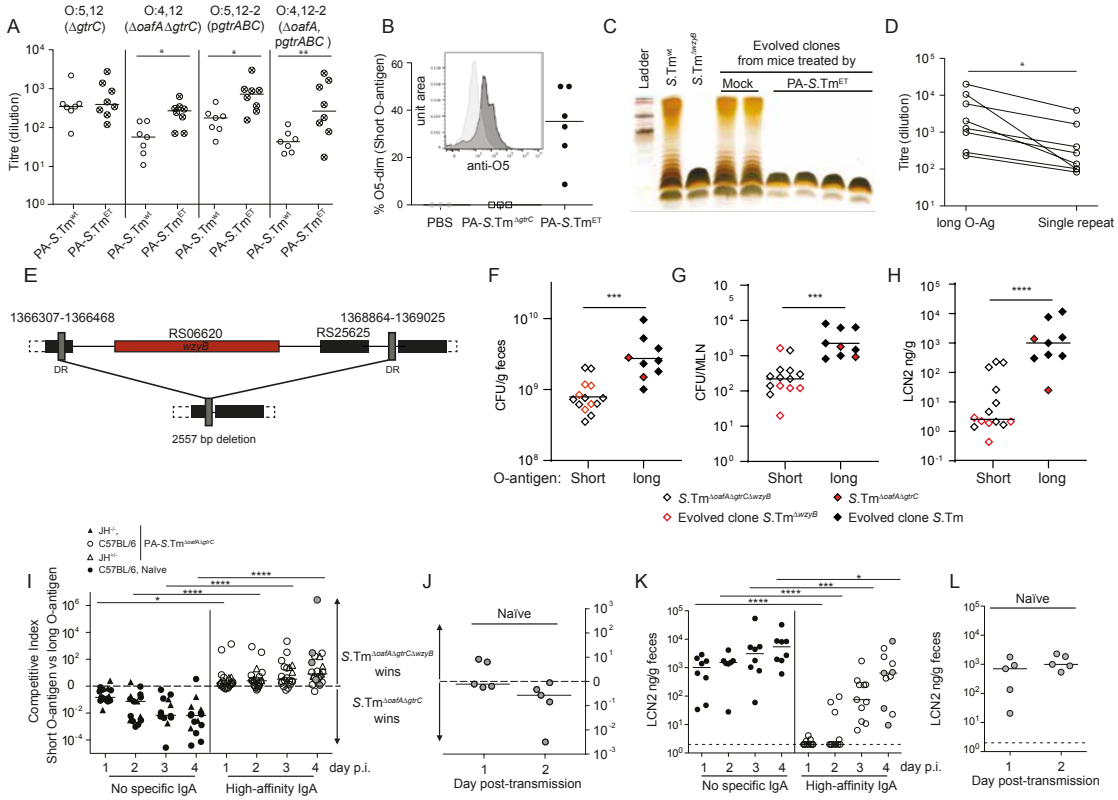

Figure 4: Vaccines combining fitness-neutral glycan variants set an evolutionary trap for *S.*Tm, selecting for strains with a single-repeat O-antigen: **A and B**. *S.*Tm clones re-isolated from the feces of mice vaccinated with PBS only, PA-*S.*Tm$^{\Delta gtrC}$ or PA-*S.*Tm^{ET} (combined PA-*S.*Tm$^{\Delta gtrC}$, PA-*S.*Tm$^{\Delta oafA\ \Delta gtrC}$, PA-*S.*Tm p*gtrABC*, and PA-*S.*Tm$^{\Delta oafA}$ p*gtrABC*). **A**. Intestinal IgA titre, determined by bacterial flow cytometry against *S.*Tm$^{\Delta gtrC}$ (O:5,12), *S.*Tm$^{\Delta oafA\ \Delta gtrC}$ (O:4,12), *S.*Tm$^{\Delta gtrC}$ p*gtrABC* (O:5, 12-2) and *S.*Tm$^{\Delta oafA\ \Delta gtrC}$ p*gtrABC* (O:4,12-2). **B**. Fraction of clones with weak anti-sera staining, as determined by flow cytometry, indicative of O-antigen shortening. One point represents one mouse. **C**. Silver-stained gel of LPS from control and evolved *S.*Tm strains from control and PA-*S.*Tm^{ET} vaccinated mice, showing short LPS in clones isolated from vaccinated PA-*S.*Tm^{ET} mice. **D**. Intestinal IgA titre from PA-*S.*Tm$^{\Delta oafA\ \Delta gtrC}$ -vaccinated mice specific for *S.*Tm $^{\Delta oafA\ \Delta gtrC}$ (long O-antigen) and *S.*Tm$^{\Delta oafA\ \Delta gtrC\ \Delta wzyB}$ (short O-antigen). **E**. Resequencing of strains with short O-antigen reveals a large genomic deletion between inverted repeats, covering the *wzyB* gene (O-antigen polymerase) n=5 clones sequenced. **F, G, H,** Single 24h infections in streptomycin pretreated naïve mice. Evolved and synthetic *wzyB* mutants have reduced ability to colonize the gut (**F**, CFU/g feces) and to spread systemically (**G**, CFU per mesenteric lymph node (MLN)). This translates into diminished propensity to trigger intestinal inflammation in comparison to *wzyB* wild type strains (**H**, fecal Lipocalin 2 (LCN2)). **I**. Mock-vaccinated wild type (C57BL/6, mock), PA-STm$^{\Delta oafA\ \Delta gtrC}$ -vaccinated JH$^{-/-}$ mice (JH$^{-/-}$, Vacc), PA-STm$^{\Delta oafA\ \Delta gtrC}$ -vaccinated wild type (C57BL/6, Vacc) and PA-STm$^{\Delta oafA\ \Delta gtrC}$ -vaccinated JH$^{+/-}$ littermate controls (JH$^{+/-}$, Vacc) mice were streptomycin pre-treated and infected with 10^5 CFU of a 1:1 ratio *S.*Tm $^{\Delta oafA\ \Delta gtrC\ \Delta wzyB}$ and *S.*Tm$^{\Delta oafA\ \Delta gtrC}$. i.e. serotype-locked, short and long O-antigen-producing strains. Competitive index of *S.*Tm in feces on the indicated days. **J**. Feces from the indicated mice (grey-filled circles) from panel **I** were transferred into streptomycin-pretreated naive mice (one fecal pellet per mouse) and competitive index in feces calculated to day 2 post-infection. **K** and **L**. Fecal Lipocalin 2 (LCN2) corresponding to panels **I** and **J** respectively. A, I, K. 2-way ANOVA on log-Normalized data. Bonferroni post-test statistics are shown. In panel I, competitive index in vaccinated mice is significantly higher than 1 at all time-points by Wilcoxon signed rank tests. D, F, G, H: Mann-Whitney U 2-tailed tests.

Supplementary Materials
Materials and methods:

Ethics statement
All animal experiments were approved by the legal authorities (licenses 223/2010, 222/2013 and 193/2016; Kantonales Veterinäramt Zürich, Switzerland) and performed according to the legal and ethical requirements.

Mice
Unless otherwise stated, all experiments used SOPF C57BL/6 mice. 129S1/SvImJ, $IgA^{-/-}$ [(*39*)], $J_H^{-/-}$ [(*40*)], $Rag1^{-/-}$ [(*41*)] (all C57BL/6 background) were re-derived into a specific opportunistic pathogen-free (SOPF) foster colony to normalize the microbiota and bred under full barrier conditions in individually ventilated cages in the ETH Phenomics center (EPIC, RCHCI), ETH Zürich. Low complex microbiota (LCM) mice (C57BL/6) are ex-germfree mice, which were colonized with a naturally diversified Altered Schaedler flora in 2007(*10*) and were bred in individually ventilated cages or flexible-film isolators at this facility. Vaccinations were started between 5 and 6 weeks of age, and males and females were randomized between groups to obtain identical ratios wherever possible. As strong phenotypes were expected, we adhered to standard practice of analysing at least 5 mice per group. Researchers were not blinded to group allocation.

Strains and plasmids
All strains and plasmids used in this study are listed **Table S1**.
For cultivation of bacteria, we used lysogeny broth (LB) containing appropriate antibiotics (i.e., 50 µg/ml streptomycin (AppliChem); 6 µg/ml chloramphenicol (AppliChem); 50 µg/ml kanamycin (AppliChem); 100 µg/ml ampicillin (AppliChem)). Dilutions were prepared in Phosphate Buffer Saline (PBS, Difco)
In-frame deletion mutants (e.g. *gtrC::cat*) were performed by *λ red* recombination as described in(*42*). When needed, antibiotic resistance cassettes were removed using the temperature-inducible FLP recombinase encoded on pCP20(*42*). Mutations coupled with antibiotic resistance cassettes were transferred into the relevant genetic background by generalized transduction with bacteriophage P22 HT105/1 *int-201*(*43*). Primers used for genetic manipulations and verifications of the constructions are listed **Table S2.** Deletions of *gtrA* and *gtrC* originated from in-frame deletions made in *S.*Tm 14028S, kind gifts from Prof. Michael McClelland (University of California, Irvine), and were transduced into the SB300 genetic background.

The *gtrABC* operon (STM0557-0559) was cloned into the pSC101 derivative plasmid pM965(*44*). The operon *gtrABC* was amplified from the chromosome of SB300 using the Phusion Polymerase (ThermoFisher Scientific) and primers listed **Table S2**. The PCR product and pM965 were digested with PstI-HF and EcoRV-HF (NEB) before kit purification (SV Gel and PCR Clean up System, Promega) and ligation in presence of T4 ligase (NEB) following manufacturer recommendations. The ligation product was transferred by electro-transformation in competent SB300 cells.

Targeted sequencing

Targeted re-sequencing by the Sanger method (Microsynth AG) was performed on kit purified PCR products (Promega) from chromosomal DNA or expression vector templates using pre-mixed sequencing primers listed **Table S2**.

Whole-genome re-sequencing of O:12^{Bimodal} isolates

The genomes of S.Tm and evolved derivatives were fully sequenced by the Miseq system (2x300bp reads, Illumina, San Diego, CA) operated at the Functional Genomic Center in Zurich. The sequence of *S*.Tm SL1344 (NC_016810.1) was used as reference. Quality check, reads trimming, alignments, SNPs and indels calling were performed using the bioinformatics software CLC Workbench (Qiagen).

Whole-genome sequencing of *S*.Tm isolates from "Evolutionary trap" vaccinated mice and variant calling.

Nextera XT libraries were prepared for each of the samples. The barcoded libraries were pooled into equimolar concentrations following manufacturer's guidelines (Illumina, San Diego, CA) using the Mid-Output Kit for paired-end sequencing (2×150 bp) on an Illumina NextSeq500 sequencing platform. Raw data (mean virtual coverage 361x) was demultiplexed and subsequently clipped of adapters using Trimmomatic v0.38 with default parameters(*45*). Quality control passing read-pairs were aligned against reference genome/plasmids (Accession numbers: NC_016810.1, NC_017718.1, NC_017719.1, NC_017720.1) with bwa v0.7.17(*46*). Genomic variant were called using Pilon v1.23(*47*). with the following parameters: (i) minimum coverage 10x; (ii) minimum quality score = 20; (iii) minimum read mapping quality = 10. SnpEff v4.3 was used to annotate variants according to NCBI and predict their effect on genes(*48*).

PA-*S*.Tm vaccinations

Peracetic acid killed vaccines were produced as previously described(*49*). Briefly, bacteria were grown overnight to late stationary phase, harvested by centrifugation and re-suspended to a density of 10^9-10^{10} per ml in sterile PBS. Peracetic acid (Sigma-Aldrich) was added to a final concentration of 0.4% v/v. The suspension was mixed thoroughly and incubated for 60 min at room temperature. Bacteria were washed once in 40 ml of sterile 10x PBS and subsequently three times in 50 ml sterile 1x PBS. The final pellet was re-suspended to yield a density of 10^{11} particles per ml in sterile PBS (determined by OD600) and stored at 4°C for up to three weeks. As a quality control, each batch of vaccine was tested before use by inoculating 100 µl of the killed vaccine (one vaccine dose) into 300 ml LB and incubating over night at 37 °C with aeration. Vaccine lots were released for use only when a negative enrichment culture had been confirmed.

Non-typhoidal *Salmonella* challenge infections

Infections were carried out as described(*50*). In order to allow reproducible gut colonization, 8-12 week-old C57Bl/6 mice, naïve or vaccinated, were orally pretreated 24 h before infection with 25 mg streptomycin. Strains were cultivated overnight separately in LB containing the appropriate antibiotics. Subcultures were prepared before infections by diluting overnight cultures 1:20 in fresh LB without antibiotics and incubation for 4 h at 37°C. The cells were washed in PBS and 50 µl of resuspended pellets were used to infect mice *per os* ($5x10^5$ CFU). Competitions were performed by inoculating 1:1 mixtures of each competitor strain.

Feces were sampled daily, homogenized in 1 ml PBS by bead beating (3mm steel ball, 25 Hz for 1 minute in a TissueLyser (Qiagen)), and *S.*Tm strains were enumerated by selective plating on MacConkey agar supplemented with the relevant antibiotics. Samples for lipocalin-2 measurements were kept homogenized in PBS at -20 °C. At endpoint, intestinal lavages were harvested by flushing the ileum content with 2 ml of PBS using a cannula. The mesenteric lymph nodes, were collected, homogenized in PBS Tergitol 0.05% v/v at 25 Hz for 2 minutes, and bacteria were enumerated by selective plating.
Competitive indexes were calculated as the ratio of relative population sizes of competitors at a given time point, normalized for the ratio in the inoculum.

Non-typhoidal *Salmonella* transmission

Donor mice were vaccinated with PA-*S.*Tm$^{\Delta oafA\ \Delta gtrC}$ once per week for 5 weeks, streptomycin pretreated (25 mg streptomycin *per os*), and gavaged 24 hours later with 10^5 CFU of a 1:1 mixture of S. Tm$^{\Delta oafA\Delta gtrCwzyB::cat}$ (Cm^R) and *S.* Tm$^{\Delta oafA\Delta gtrC\ \mathrm{Kan}}$ (Kan^R). On day 4 post infection, the donor mice were euthanized, organs were harvested, and fecal pellets were collected, weighed and homogenized in 1 ml of PBS. The re-suspended feces (centrifuged for 10 seconds to discard large debris) were immediately used to gavage (as a 50 µl volume containing the bacteria from on fecal pellet) recipient naïve mice (pretreated with 25 mg streptomycin 24 hours before infection). Recipient mice were euthanized and organs were collected on day 2 post transmission. In both donor and recipient mice, fecal pellets were collected daily and selective plating was used to enumerate *Salmonella* and determine the relative proportions (and consequently the competitive index) of both competing bacterial strains.

Quantification of fecal Lipocalin2

Fecal pellets collected at the indicated time-points were homogenized in PBS by bead-beating at 25 Hz, 1min. Large particles were sedimented by centrifugation at 300 g, 1min. The resulting supernatant was then analysed in serial dilution using the mouse Lipocalin2 ELISA duoset (R&D) according to the manufacturer's instructions.

Analysis of IgA-coating, and O:5/O:12 expression on *S.*Tm in cecal content

Fresh cecal content or feces was re-suspended in sterile PBS by bead-beating at 25 Hz, 1min (previously demonstrated to disrupt IgA cross-linked clumps(*9*)). An aliquot estimated to contain not more than 10^6 *S.*Tm was directly stained with a monoclonal human IgG-anti-O:12 (STA5(*9*)) and biotin-conjugated anti-mouse IgA clone RMA-1 (Biolegend), and/or Rabbit-anti-*Salmonella* O:5 (Difco). After washing, secondary reagents Alex647-anti-human IgG (Jackson Immunoresearch), Pacific Blue-conjugated streptavidin (Molecular Probes), Phycoerythrin-conjugated streptavadin (Molecular Probes) and/or Brilliant violet 421-anti-Rabbit IgG (Biolegend) were added. After a final washing step, samples were analysed on a BD LSRII flow cytometer, or a Beckman Coulter Cytoflex S, with settings adapted for optimal detection of bacterial-sized particles. The median fluorescence intensity of IgA staining on *S.*Tm was determined by "gating" on bacterial sized particles and calculating the appropriate median fluoresence corresponding to O:12 or O:5 staining FlowJo (Treestar, USA). Gates used to calculate the % of "ON" and "OFF" cells were calculated by gating on samples with known ON or OFF phenotypes.

Analysis of specific antibody titers by bacterial flow cytometry

141 Specific antibody titers in mouse intestinal washes were measured by flow cytometry as
142 described(*9*, *51*). Briefly, intestinal washes were collected by flushing the small intestine with
143 5ml PBS, centrifuged at 16000 g for 30 min and aliquots of the supernatants were stored at -
144 20°C until analysis. Bacterial targets (antigen against which antibodies are to be titered) were
145 grown to late stationary phase or the required OD, then gently pelleted for 2 min at 3000 g.
146 The pellet was washed with sterile-filtered 1% BSA/PBS before re-suspending at a density of
147 approximately 10^7 bacteria per ml. After thawing, intestinal washes were centrifuged again at
148 16000 g for 10 min. Supernatants were used to perform serial dilutions. 25 µl of the dilutions
149 were incubated with 25 µl bacterial suspension at 4°C for 1h. Bacteria were washed twice
150 with 200 µl 1% BSA/PBS before resuspending in 25 µl 1% BSA/PBS containing monoclonal
151 FITC-anti-mouse IgA (BD Pharmingen, 10µg/ml) or Brilliant violet 421-anti-IgA (BD
152 Pharmingen). After 1h of incubation, bacteria were washed once with 1% BSA/PBS and
153 resuspended in 300µl 1% BSA/PBS for acquisition on LSRII or Beckman Coulter Cytoflex S
154 using FSC and SSC parameters in logarithmic mode. Data were analysed using FloJo
155 (Treestar). After gating on bacterial particles, log-median fluorescence intensities (MFI) were
156 plotted against antibody concentrations for each sample and 4-parameter logistic curves were
157 fitted using Prism (Graphpad, USA). Titers were calculated from these curves as the inverse
158 of the antibody concentration giving an above-background signal.
159
160 **Flow cytometry for analysis of O:5, O:4 and O:12 epitope abundance on *Salmonella* in**
161 **cecal content, enrichment cultures and clonal cultures**
162 1µl of overnight cultures, or 1µl of fresh feces or cecal content suspension (as above) was
163 stained with STA5 (human recombinant monoclonal IgG2 anti-O:12(*9*)), Rabbit anti-
164 *Salmonella* O:5 or Rabbit anti-*Salmonella* O:4. After incubation at 4°C for 30 min, bacteria
165 were washed once with PBS/1% BSA and resuspended in appropriate secondary reagents
166 (Alexa 647-anti-human IgG, Jackson Immunoresearch, Brilliant Violet 421-anti-Rabbit IgG,
167 Biolegend). This was incubated for 10-60 min before cells were washed and resuspended for
168 acquisition on a BD LSRII or Beckman Coulter Cytoflex S.
169
170 **Live-cell immunofluorescence**
171 200 uL of an overnight culture was centrifuged and resuspended in 200 µL PBS containing 1
172 µg recombinant murine IgA clone STA121-AlexaFluor568. The cells and antibodies were
173 co-incubated for 20 minutes at room temperature in the dark and then washed twice in 1 mL
174 Lysogeny broth (LB). Antibody-labeled cells were pipetted into in-house fabricated
175 microfluidic device(*52*). Cells in the microfluidic device were continuously fed S.Tm-
176 conditioned LB(*52*) containing STA121-AlexaFluor568 (1 µg/mL). Media was flowed
177 through the device at a flow rate of 0.2 mL/h using syringe pumps (NE-300, NewEra
178 PumpSystems). Cells in the microfluidic device were imaged on an automated Olympus IX81
179 microscope enclosed in an incubation chamber heated to 37°C. At least 10 unique positions
180 were monitored in parallel per experiment. Phase contrast and fluorescence images were
181 acquired every 3 minutes. Images were deconvoluted in MatLab(*53*). Videos are compressed
182 to 7 fps, i.e. 1 s = 21 mins.
183
184 **HR-MAS NMR**
185 *S*. Typhimurium cells were grown overnight (~18h) a to late stationary phase. The equivalent
186 of 11–15 OD_{600} was pelleted by centrifugation for 10 min 4 °C and 3750 *g*. The pellet was
187 resuspended in 10% NaN_3 in potassium phosphate buffer (PPB; 10 mM pH 7.4) in D_2O and

188 incubated at room temperature for at least 90 min. The cells were then washed twice with
189 PPB and resuspended in PPB to a final concentration of 0.2 OD_{600}/µl in PPB containing
190 acetone (final concentration 0.1% (v/v) as internal reference. The samples were kept on ice
191 until the NMR measurements were performed - i.e. for between 1 and 8 h. The HR-MAS
192 NMR spectra were recorded in two batches, as follows: $S.Tm^{WT}$, $S.Tm^{wbaP}$, $S.Tm^{Evolved_1}$,
193 $S.Tm^{Evolved_2}$ were measured on 16.12.2016, $S.Tm^{OafA}$ was measured on 26.7.17.
194
195 NMR experiments on intact cells were carried out on a Bruker Biospin AVANCE III
196 spectrometer operating at 600 MHz ^{1}H Larmor frequency using a 4 mm HR-MAS Bruker
197 probe with 50 µl restricted-volume rotors. Spectra were collected at a temperature of 27 °C
198 and a spinning frequency of 3 kHz except for the sample of OafA (25 °C, 2 kHz). The ^{1}H
199 experiments were performed with a 24 ms Carr–Purcell–Meiboom–Gill (CPMG) pulse-
200 sequence with rotor synchronous refocusing pulses every two rotor periods before acquisition
201 of the last echo signal to remove broad lines due to solid-like material(*27*). The 90° pulse was
202 set to 6.5 µs, the acquisition time was 1.36 s, the spectral width to 20 ppm. The signal of
203 HDO was attenuated using water presaturation for 2 s. 400 scans were recorded in a total
204 experimental time of about 30 minutes.
205
206 **O-Antigen purification and ^{1}H-NMR**
207 The LPS was isolated applying the hot phenol-water method(*54*), followed by dialysis against
208 distilled water until the phenol scent was gone. Then samples were treated with DNase
209 (1mg/100 mg LPS) plus RNase (2 mg/100 mg LPS) at 37°C for 2 h, followed by Proteinase K
210 treatment (1 mg/100 mg LPS) at 60°C for 1 h [all enzymes from Serva, Germany].
211 Subsequently, samples were dialyzed again for 2 more days, then freeze dried. Such LPS
212 samples were then hydrolyzed with 1% aqueous acetic acid (100°C, 90 min) and ultra-
213 centrifuged for 16 h at 4°C and 150,000 *g*. Resulting supernatants (the O-antigens) were
214 dissolved in water and freeze-dried. For further purification, the crude O-antigen samples
215 were chromatographed on TSK HW-40 eluted with pyridine/acetic acid/water (10/4/1000, by
216 vol.), then lyophilized. On these samples, 1D and 2 D (COSY, TOCSY, HSQC, HMBC) ^{1}H-
217 and ^{13}C-NMR spectra were recorded with a Bruker DRX Avance 700 MHz spectrometer (^{1}H:
218 700.75 MHz; ^{13}C: 176.2 MHz) as described(*55*).
219
220 **Atomic force microscopy**
221 The indicated S.Tm strains were grown to late-log phase, pelleted, washed once with distilled
222 water to remove salt. A 20 µl of bacterial solution was deposited onto freshly cleaved mica,
223 adsorbed for 1 min and dried under a clean airstream. The surface of bacteria was probed
224 using a Dimension FastScan Bio microscope (Bruker) with Bruker AFM cantilevers in
225 tapping mode under ambient conditions. The microscope was covered with an acoustic hood
226 to minimized vibrational noise. AFM images were analyzed using the Nanoscope Analysis
227 1.5 software.
228
229 **Methylation analysis of S.Tm clones**
230 For REC-Seq (restriction enzyme cleavage–sequencing) we followed the same procedure
231 described by Ardissone et al, 2016(*56*). In brief, 1 µg of genomic DNA from each S.Tm was
232 cleaved with MboI, a blocked (5'biotinylated) specific adaptor was ligated to the ends and the
233 ligated fragments were then sheared to an average size of 150-400 bp (Fasteris SA, Geneva,
234 CH). Illumina adaptors were then ligated to the sheared ends followed by deep-sequencing

235 using a HiSeq Illumina sequencer, the 50 bp single end reads were quality controlled with
236 FastQC (http://www.bioinformatics.babraham.ac.uk/projects/fastqc/). To remove
237 contaminating sequences, the reads were split according to the MboI consensus motif (5'-
238 ^GATC-3') considered as a barcode sequence using fastx_toolkit
239 (http://hannonlab.cshl.edu/fastx_toolkit/) (fastx_barcode_splitter.pl --bcfile barcodelist.txt --
240 bol --exact). A large part of the reads (60%) were rejected and 40% kept for remapping to the
241 reference genomes with bwa mem(*46*) and samtools(*57*) to generate a sorted bam file. The
242 bam file was further filtered to remove low mapping quality reads (keeping AS >= 45) and
243 split by orientation (alignmentFlag 0 or 16) with bamtools(*58*). The reads were counted at 5'
244 positions using Bedtools(*59*) (bedtools genomecov -d -5). Both orientation count files were
245 combined into a bed file at each identified 5'-GATC-3' motif using a home-made PERL
246 script. The MboI positions in the bed file were associated with the closest gene using
247 Bedtools closest(*59*) and the gff3 file of the reference genomes(*60*). The final bed file was
248 converted to an MS Excel sheet with a homemade script. The counts were loaded in RStudio
249 1.1.442(*61*) with R version 3.4.4(*62*) and analysed with the DESeq2 1.18.1 package(*63*)
250 comparing the reference strain with the 3 evolved strains considered as replicates. The counts
251 are analysed by genome position rather than by gene. The positions are considered
252 significantly differentially methylated upon an adjusted p-value < 0.05. Of the 2607 GATC
253 positions, only 4 were found significantly differentially methylated and they are all located in
254 the promoter of the gtrABC operon.
255
256 ***gtrABC* expression analysis by blue/white screening and flow cytometry.**
257 About 200 colonies of *S*.Tm$^{gtrABC\text{-}lacZ}$ (strain background 4/74, (*22*)) were grown from an
258 overnight culture on LB agar supplemented with X-gal (0.2 mg/ml, Sigma) in order to select
259 for *gtrABC* ON (blue) and OFF clones (white). These colonies were then picked to start pure
260 overnight cultures. These cultures were diluted and plated on fresh LB agar X-gal plate in
261 order to enumerate the proportion of *gtrABC* ON and OFF siblings. The proportion of
262 O:12/O:12-2 cells was analyzed by flow cytometry.
263
264 ***In vitro* growth and competitions to determine *wzyB*-associated fitness costs**
265 Single or 1:1 mixed LB subcultures were diluted 1000 times in 200 µl of media distributed in
266 96 well Black side microplates (Costar). Where appropriate, wild type *S*.Tm carried a plasmid
267 for constitutive expression of GFP. To measure growth and competitions in stressful
268 conditions that specifically destabilize the outer membrane of *S*.Tm, a mixture of Tris and
269 EDTA (Sigma) was diluted to final concentration (4 mM Tris, 0.4 mM EDTA) in LB. The
270 lid-closed microplates were incubated at 37°C with fast and continuous shaking in a
271 microplate reader (Synergy H4, BioTek Instruments). The optical density was measured at
272 600 nm and the green fluorescence using 491 nm excitation and 512 nm emission filter
273 wavelengths every 10 minutes for 18 h. The outcome of competitions was determined by
274 calculating mean OD and fluorescence intensity measured during the last 100 min of
275 incubation. OD and fluorescence values were corrected for the baseline value measured at
276 time 0.
277
278 **Serum resistance**
279 Overnight LB cultures were washed three times in PBS, OD adjusted to 0.5 and incubated
280 with pooled human serum obtained from Unispital Basel (3 vol of culture for 1 vol of serum)
281 at 37°C for 1 h. Heat inactivated (56°C, 30 min) serum was used as control treatment.

Surviving bacteria were enumerated by plating on non-selective LB agar plates. For this, dilutions were prepared in PBS immediately after incubation.

Modeling antigen switching between O12 and O12-2

The aim of this modeling approach is to test whether a constant switching rate between an O12 and an O12-2 antigen expression state can explain the experimentally observed bimodal populations.

To this end, we formulated a deterministic model of population dynamics of the two phenotypic states as

$$\frac{dO_{12}}{dt} = (\mu O_{12} - s_{\rightarrow 12-2} O_{12} + s_{\rightarrow 12} O_{12-2}) * \left(1 - \frac{(O_{12} + O_{12-2})}{K}\right)$$

$$\frac{dO_{12-2}}{dt} = (\mu O_{12-2} + s_{\rightarrow 12-2} O_{12} - s_{\rightarrow 12} O_{12-2}) * \left(1 - \frac{(O_{12} + O_{12-2})}{K}\right),$$

where O_{12} and O_{12-2} denote the population sizes of the respective antigen variants, μ denotes the growth rate, which is assumed to be identical for the two variants, K the carrying capacity, and $s_{\rightarrow 12-2}$ and $s_{\rightarrow 12}$ the respective switching rates from O_{12} to O_{12-2} and from O_{12-2} to O_{12}.Growth, as well as the antigen switching rates, are scaled with population size in a logistic way, so that all processes come to a halt when carrying capacity is reached.

We use the model to predict the composition of a population after growth in LB overnight, and therefore set the specific growth rate to $\mu = 2.05h^{-1}$, which corresponds to a doubling time of roughly 20min. The carrying capacity is set to $K = 10^9\ cells$. We ran parameter scans for the switching rates $s_{\rightarrow 12}$ and $s_{\rightarrow 12-2}$, with population compositions that start either with 100% or 0% O_{12}, and measure the composition of the population after 16h of growth (**Fig. S4C**). The initial population size is set to $10^4\ cells$

Experimentally, we observe that when starting a culture with an O_{12} colony, after overnight growth the culture is composed of around 90% O_{12} and 10% O_{12-2} cells, whereas starting the culture with O_{12-2} cells yields around 50% O_{12} and 50% O_{12-2} cells after overnight growth (**Fig. S4B**). To explain this observation without a change in switching rates, we would need a combination of values in $s_{\rightarrow 12}$ and $s_{\rightarrow 12-2}$ that yield the correct population composition for both scenarios. In **Fig. S4D**, we plot the values of $s_{\rightarrow 12}$ and $s_{\rightarrow 12-2}$ that yield values of 10% O_{12-2} (starting with 0% O_{12-2}, green dots) and 50% O_{12-2} (starting with 100% O_{12-2}, orange dots). The point clusters intersect at $s_{\rightarrow 12} = 0.144h^{-1}$ and $s_{\rightarrow 12-2} = 0.037h^{-1}$ (as determined by a local linear regression at the intersection point).

We then used the thus determined switching rates to produce a population growth curve in a in a deterministic simulation, using the above equations for a cultures starting with 100% O_{12-2}, (**Fig. S4E**, Left-hand graph) and for a culture starting with 0% O_{12-2} (Fig. S4E, right-hand graph).

These switching rates are consistent with published values (*22*). Our results show that the observed phenotype distributions can be explained without a change in the rate of switching between the phenotypes.

Key to O-glycan repeat structures in this manuscript

Serovar	Full Representation	SNFG Representation
O:5,12	O:5 Abe(2--Ac) α1 3 -2)-D-Man-(α1-4)-L-Rha-(α1-3)-D-Gal-(α1- O:12	
O:4,12	O:12-2 D-Glu α1 4 O:4 Abe α1 3 -2)-D-Man-(α1-4)-L-Rha-(α1-3)-D-Gal-(α1- O:12	
O:5,12-2	O:5 Abe(2--Ac) α1 3 O:12-2 D-Glu α1 4 -2)-D-Man-(α1-4)-L-Rha-(α1-3)-D-Gal-(α1-	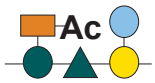
O:4,12-2	O:12-2 O:4 Abe α1 3 D-Glu α1 4 -2)-D-Man-(α1-4)-L-Rha-(α1-3)-D-Gal-(α1-	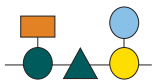

Supplementary Figures 1 - 11

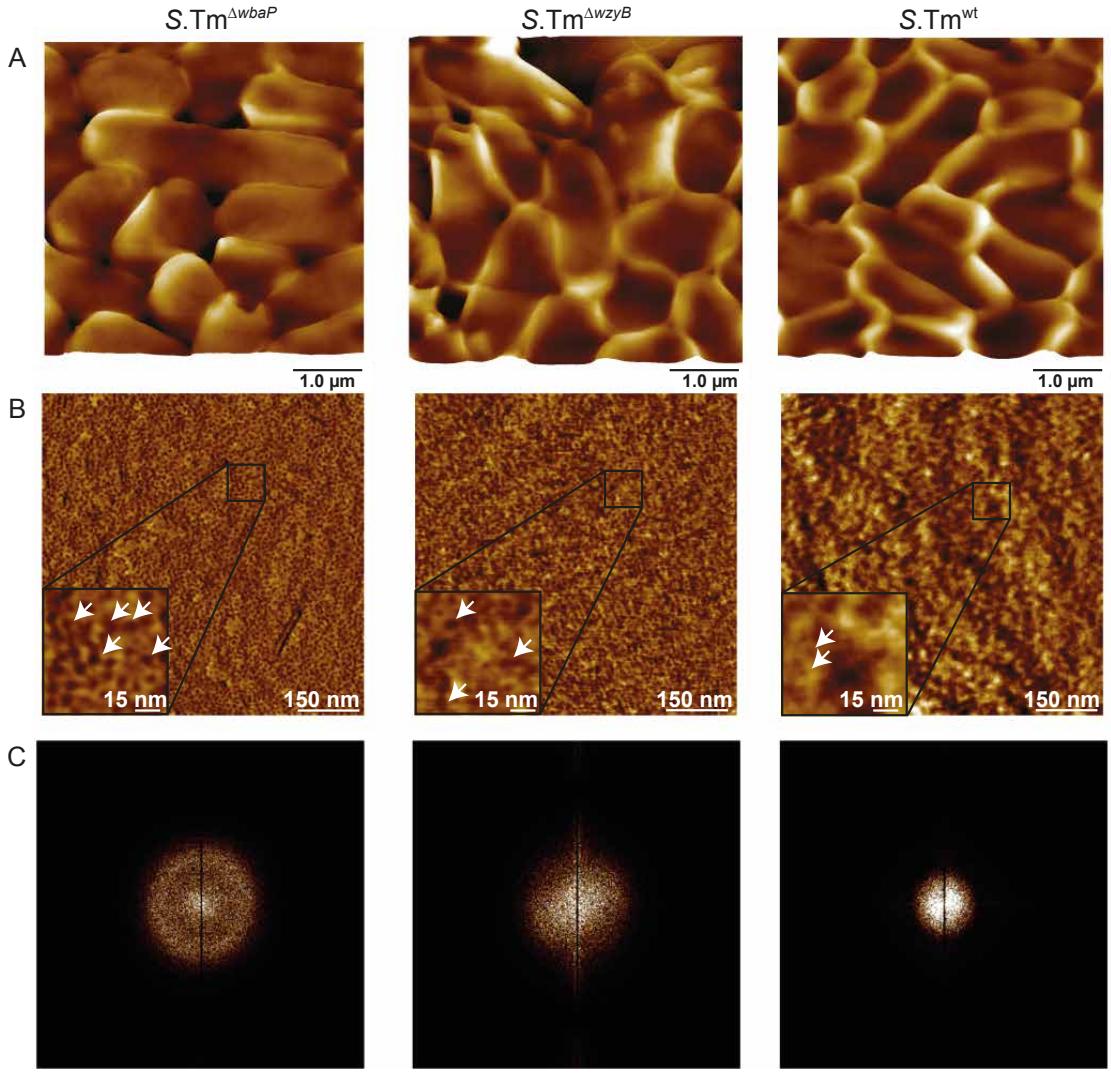

Fig. S1: Surface phenotype of *S.*Tm mutants: **A-C**. Atomic force microscopy phase images of *S.*Tm^{wt}, *S.*Tm$^{\Delta wzyB}$ (single-repeat O-antigen), and *S.*Tm$^{\Delta wbaP}$ (rough mutant - no O-antigen) at low magnification (A) and high magnification (B and C). Invaginations in the surface of *S.*Tm$^{\Delta wbaP}$ (dark colour, B) show a geometry and size consistent with outer membrane pores(*64*). These are already less clearly visible on the surface of *S.*Tm$^{\Delta wzyB}$ with a single-repeat O-antigen, and become very difficult to discern in *S.*Tm^{wt}. **C**. Fast-Fourier transform of images shown in "B" demonstrating clear regularity on the surface of *S.*Tm$^{\Delta wbaP}$, which is progressively lost when short and long O-antigen is present.

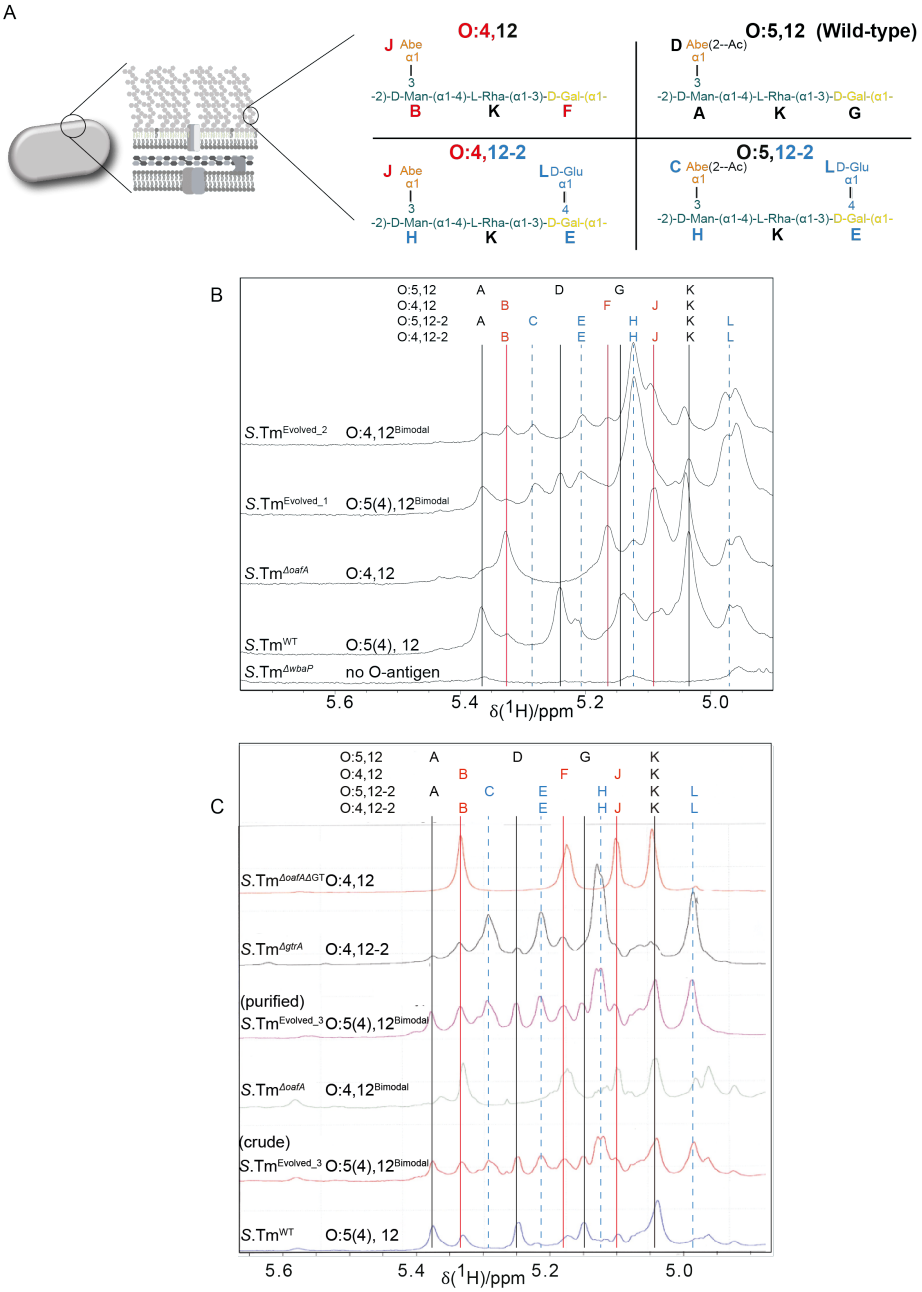

Fig. S2: NMR of purified LPS from the indicated strains. A. Schematic diagram of expected NMR peaks for each molecular species **B.** HR-MAS ^{1}H-NMR spectra. Spectra show predicted peak positions, and observed spectra for C1 protons of the O-antigen sugars. **C.** ^{1}H NMR of purified LPS from the indicated strains. Note that non-acetylated Abequose can be observed in wild-type strains due to spontaneous deacetylation at low pH in late stationary phase cultures(*27*). A *gtrA* mutant strain is used here to over-represent the O:12-2 O-antigen variant due to loss of regulation(*31*).

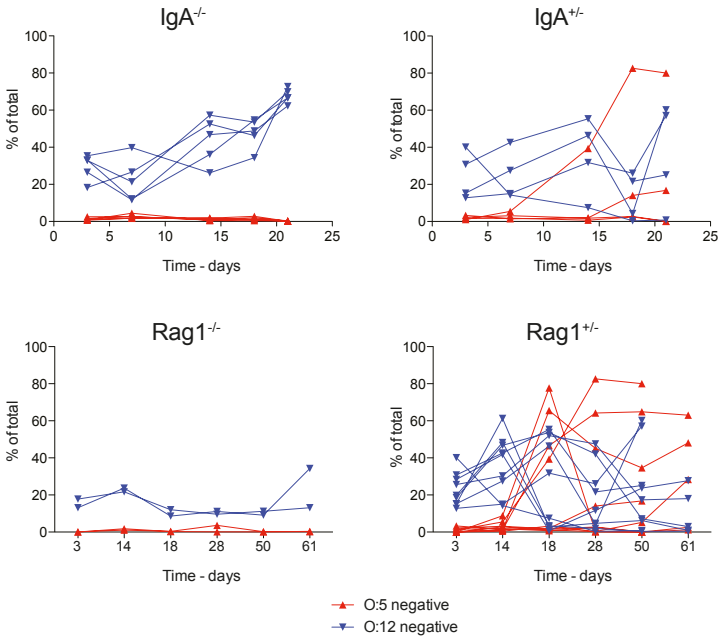

Fig. S3: *S*.Tm O-antigen variation occurs in chronic *S*.Tm infections in an antibody-dependent manner. IgA$^{-/-}$ and Rag1$^{-/-}$ and heterozygote littermate controls were pre-treated with streptomycin and infected with *S*.Tm$^{\Delta sseD}$ orally. Feces were collected at the indicated time-points, enriched overnight in LB plus kanamycin, stained for O:5 and O:12 and analysed by flow cytometry. The fraction of the population that lost O:5 and O:12 antisera staining is shown over time. Outgrowth of O:12-negative *S*.Tm clones in IgA-deficient mice is likely due to weak compensatory responses from remaining adaptive immune mechanisms, e.g. IgM.

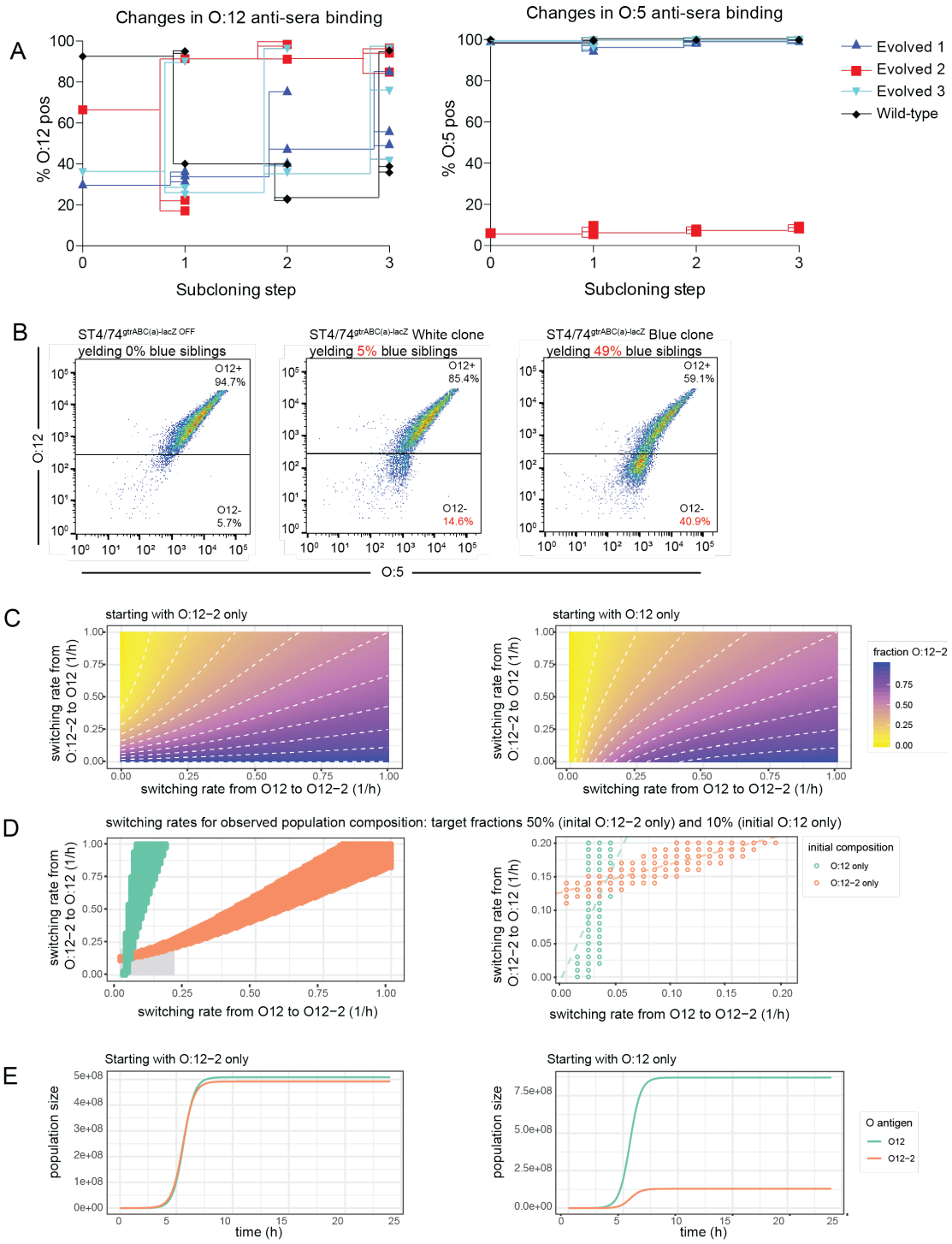

Fig. S4: Loss of O:12-staining is a reversible phenotype. A. Wild type and evolved *S.*Tm clones were picked from LB plates, cultured overnight, phenotypically characterized by O:12 (left panel) and O:5 staining (right panel), plated and re-picked. This process was repeated over 3 cycles with lines showing the descendants of each clone. **B**. Comparison of fractions of O:12-positive and O:12-negative bacteria (in fact O:12-2) determined by flow cytometry staining with typing sera and by blue-white colony counts using a *gtrABC-lacZ* reporter strain. **C-E**. Results of a mathematical model simulating bacterial growth and antigen switching. **C.** Switching rates from O:12 to O:12-2 and from O:12-2 to O:12 were varied computationally, and the fraction of O:12-2 was plotted after 16h of growth. Left-hand plot depicts the results of the deterministic model when starting with 100% O:12-2, right-hand plot depicts the results when starting with 100% O:12. **D.** depicts only the switching rates that comply with the experimentally observed antigen ratios after overnight growth (90% O12

when starting with O:12, and 50% O:12 when starting with O:12-2). Right-hand plot is a zoomed version showing values for switching rates between 0 – 0.1 h^{-1} (marked by a grey rectangle in **D.** left-hand plot. Dashed lines are linear regressions on the values in this range, and their intersection marks the switching rates used for the stochastic simulation in (E). **E**. Simulation results of bacterial population growth, when starting with only O:12-2 (left-hand plot) or only O:12 (right-hand plot). $\mu = 2.05h^{-1}$ was kept constant in all simulations; switching rates were varied in steps of $0.01h^{-1}$ in (C and D), and kept constant at $s_{\rightarrow 12} = 0.144h^{-1}$ and $s_{\rightarrow 12-2} = 0.0365h^{-1}$ in (E); the starting populations were always $10^4 cells$ individuals of the indicated phenotype; carrying capacity was always $K = 10^9 cells$. Time resolution for the simulations is $0.2h$.

Fig. S5: Mutations detected in the *oafA* gene sequence among several strains of *S.* Tm A. Aligned fractions of the *oafA* ORF from a natural isolate (from chicken) presenting the same 7 bp deletion detected in mutants of *S*.Tm SL1344 emerging in vaccinated mice. *S*. Tm SL1344 was used a reference(*65*). **B**. Aligned *oafA* promoter sequences from three natural isolates of human origin (stool or cerebrospinal fluid(*66*)) showing variations in the number of 9 bp direct repeats.

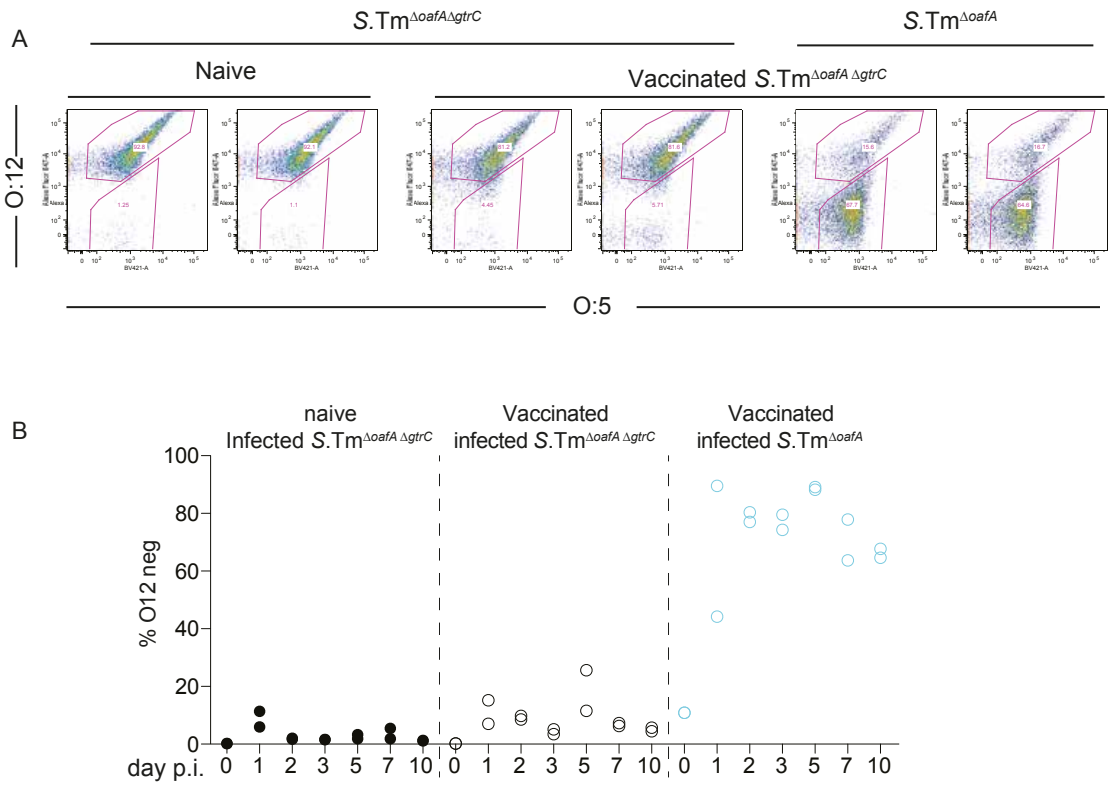

Fig. S6: Glucosyltransferases containing loci including *gtrABC* are required for generation of the O:12^{Biomodal} phenotype: Wild type 129Sv mice were mock-vaccinated or were vaccinated with PA-*S.*Tm$^{\Delta oafA\ \Delta gtrC}$ as in Fig. 1A. On d28, all mice were pre-treated with streptomycin, and infected with the indicated strain. A. Feces recovered at day 10 post-infection, was enriched overnight by culture in streptomycin, and stained for O:12. Fraction O:12-low *S.*Tm was determined by flow cytometry. Percentage of *S.*Tm that are O:12-negative was quantifed over 10 days and is plotted in panel B.

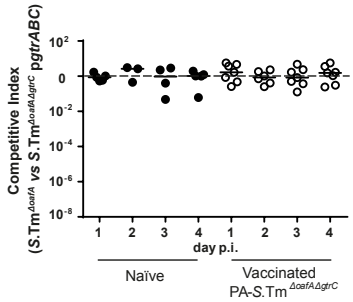

Fig. S7: The Δ*gtrC* mutation can be complemented in trans: Mice were vaccinated and pre-treated as in **Fig. 3**. The inoculum contained a 1:1 ratio of *S.*Tm$^{\Delta oafA}$ and *S.*Tm$^{\Delta oafA\ \Delta gtrC}$ p*gtrABC*. Competitive index in feces was determined by differential selective plating over 4 days post-infection.

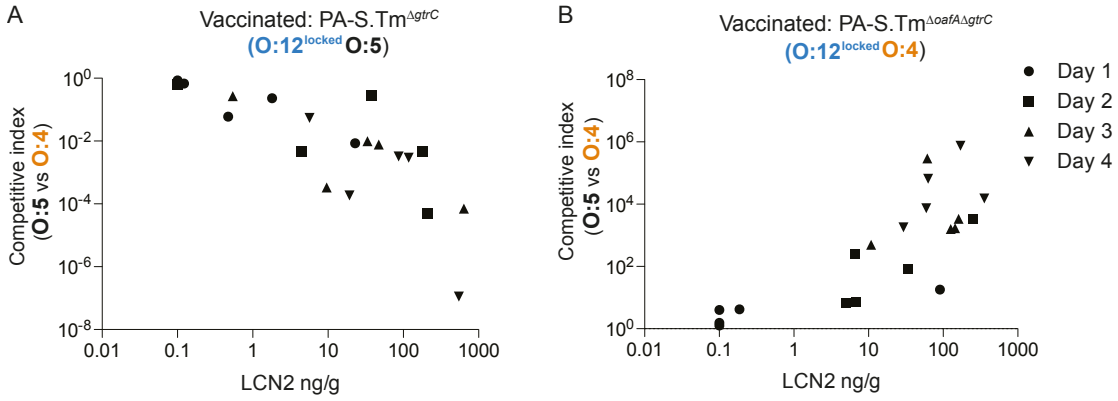

Fig. S8: Fecal lipocalin-2 measurements corresponding to Fig. 3A. Fecal Lipocalin 2 (LCN2) over days 1-4 plotted against the competitive index of infection for animals from Fig. 3A, vaccinated either against O:5-producing *S.*Tm (A), or O:4-producing *S.*Tm (B). Symbols indicate different days post-infection as indicated in the legend.

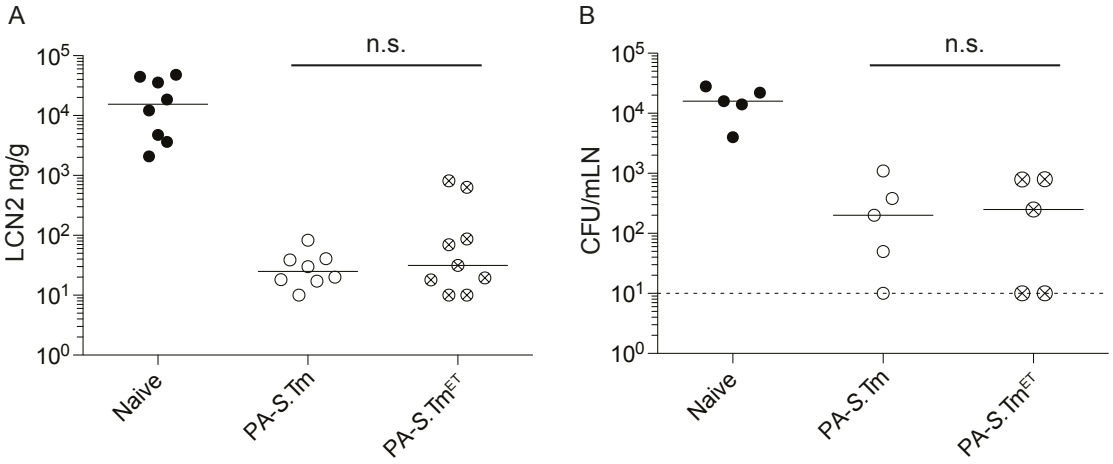

Fig. S9: PA-STm^{ET} does not significantly increase protection over a wild type vaccine at day 4 post-infection. Mice were vaccinated with vehicle only (Naïve), PA-S.Tm^{wt} of PA-STm^{ET} (combined PA-*S.*Tm$^{\Delta gtrC}$, PA-*S.*Tm$^{\Delta oafA\ \Delta gtrC}$, PA-*S.*Tm p*gtrABC*, and PA-*S.*Tm$^{\Delta oafA}$ p*gtrABC*, IgA titres shown in **Fig. 4A**). On day 28 after the first vaccination, mice were streptomycin pre-treated and challenged with 10^5 *S.*Tm^{wt} orally. Fecal Lipocalin-2 (LCN2) at day 4 post-infection (**A**) and CFU *S.*Tm^{wt} per mesenteric lymph node (MLN) at day 4 post-infection (**B**). Kruskal-Wallis analyses were carried out for significance.

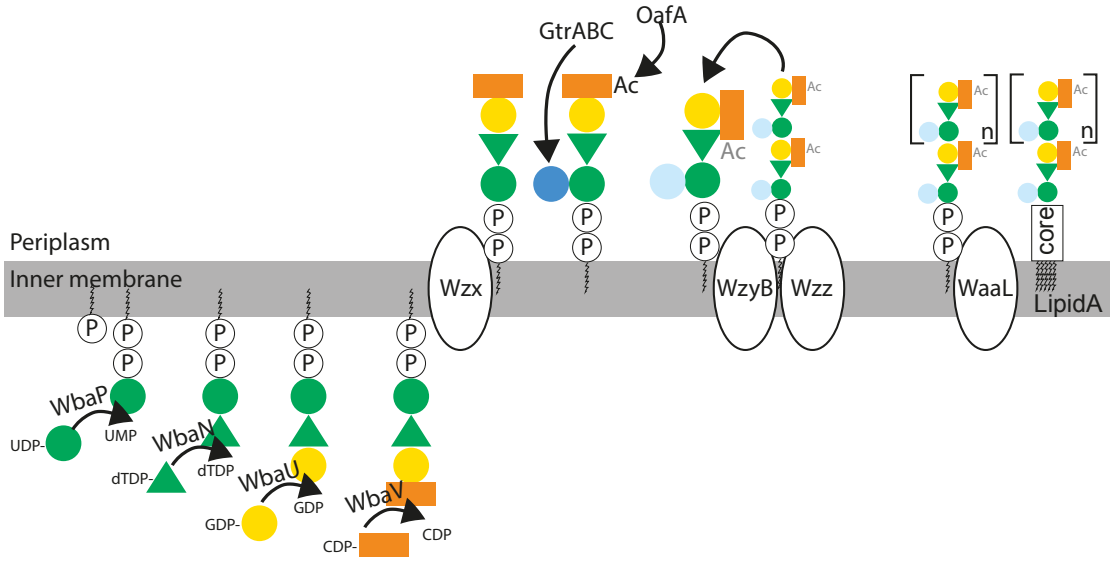

Fig. S10: Schematic of *S.*Tm O-antigen synthesis (based on(*67*))

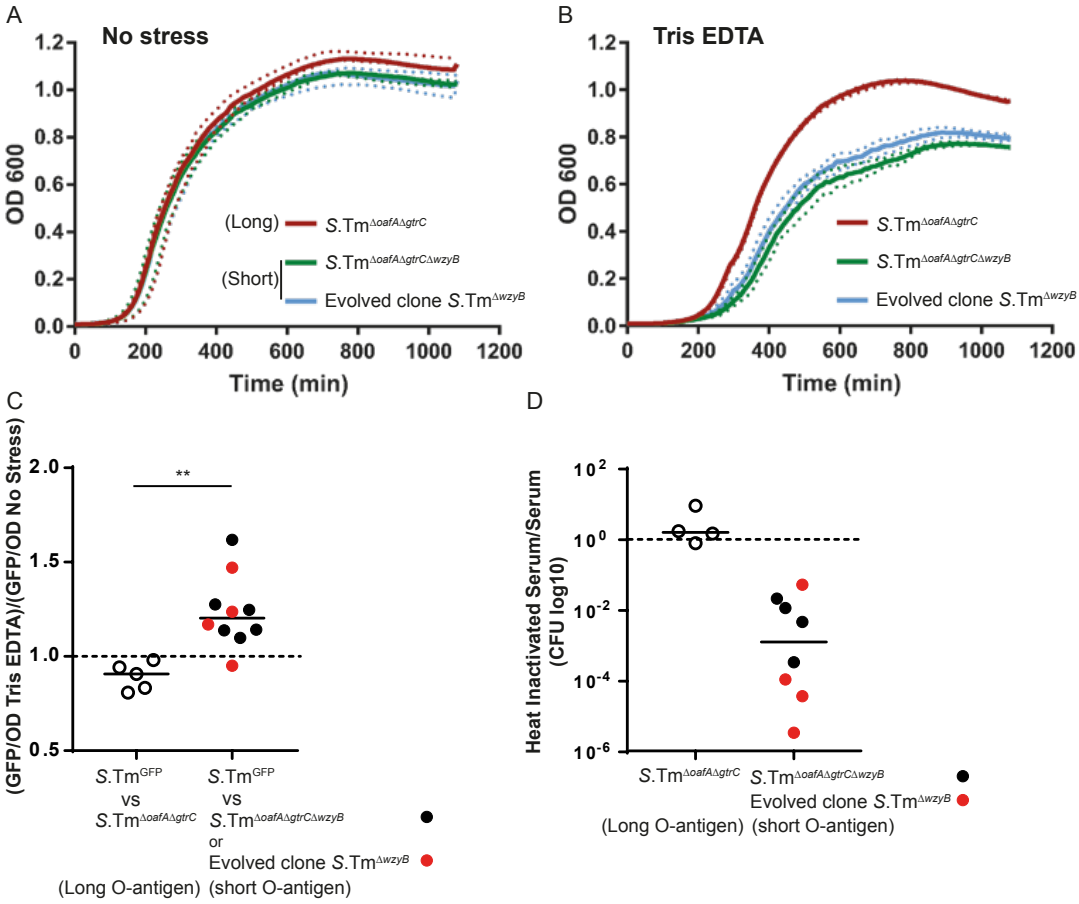

Fig. S11 Synthetic and natural deletions of *wzyB* reduce the fitness of *S*.Tm in presence of Tris-EDTA and serum complement. The deletion of *wzyB* does not affect the growth of *S*.Tm or *S*.Tm$^{\Delta oafA\ \Delta gtrC}$ in LB (No stress) **(A)** but impairs growth in presence of Tris-EDTA **(B).** Dashed lines represent the range of variations between experiments. This was in line with the outcome of competitions between *S*.Tm expressing constitutive Green Fluorescent Protein (*S*.Tm^{GFP}) and *S*.Tm $^{\Delta oafA\ \Delta gtrC\ \Delta wzyB}$ or a *wzyB* mutant isolated from an Evoltrap vaccinated mouse **(C)**. The level of GFP corrected for the optical density (OD) served as readout to quantify the *S*.Tm^{GFP} population at the end of the overnight growth, in presence of S.Tm$^{\Delta oafA\ \Delta gtrC}$, S.Tm $^{\Delta oafA\ \Delta gtrC\ \Delta wzyB}$ or an evolved *S*.Tm$^{\Delta wzyB}$, in LB with or without Tris-EDTA. Values above 1 (dashed line) indicates that relatively more GFP was detected in presence of Tris-EDTA than without, which resulted from a competitive advantage of *S*.Tm^{GFP} in presence of stress. **D**. The deletion of *wzyB* makes *Salmonella* sensitive to human serum complement. Values below 10^0 (dashed line) indicates that the number of colony-forming units (CFU) detected after incubation in human serum was lower than after incubation in heat inactivated human serum.

Supplementary Movies A and B

Visualization of O:12 phase variation using live-cell immunofluorescence. Cells expressing GFP (green) pre-stained with fluorescently-labeled recombinant murine IgA STA121 specific for the O:12 epitope (red) were loaded into a microfluidic chip for time-lapse microscopy. Cells were fed continuously S.Tm-conditioned LB containing fluorescently-labeled recombinant murine IgA STA121 specific for the O:12 epitope. (A) Loss and (B) gain of antibody reactivity (red staining) was observed, indicative of O:12 phase variation.

Supplementary Table 1: Strains and plasmids used in this study

Strains	Background	Relevant genotype	Resistance*	Reference
S.Tm^{WT}	SL1344	Wild-Type strain SB300	Sm	***Hoiseth 1981***(*68*)
S.Tm$^{\Delta sseD}$	SB300	*sseD::aphT*	Sm, Kan	***Hapfelmeier 2005***(*69*)
S.Tm$^{\Delta oafA}$	SB300	*ΔoafA* Tag1*::aphT*	Sm, Kan	This work
S.Tm$^{\Delta gtrC}$	SB300	*gtrC(a)::cat*	Sm, Cm	This work
S.Tm$^{\Delta gtrA}$	SB300	*gtrA(a)::cat*	Sm, Cm	This work
S.Tm$^{\Delta oafA\ \Delta gtrC}$	SB300	*ΔoafA gtrC(a)::cat*	Sm, Cm	This work
S.Tm$^{\Delta oafA\ \Delta gtrC\ kan}$	SB300	*ΔoafA gtrC(a)*Tag1*::aphT*	Sm, Kan	This work
S.Tm$^{\Delta oafA\ \Delta gtrC\ \Delta wzyB}$	SB300	*ΔoafA gtrC(a) wzyB::cat*	Sm, Cm	This work
S.Tm$^{\Delta oafA\ \Delta GT}$	SB300	*ΔoafA ΔgtrB(a) ΔgtrB(b) ΔSTM0712-0723 Δwca-wza*	Sm	This work
S.Tm$^{gtrABC\text{-}lacZ}$	ST4/74	*gtrABC(a)-lacZ*		***Broadbent 2010 (22)***
S.Tm$^{gtrABC\text{-}lacZ\ OFF}$	ST4/74	*gtrABC(a)-lacZ;* 3rd GTAC->GATA; 4th GATC->GATT		***Broadbent 2010 (22)***
S.Tm$^{\Delta oafA\ \Delta gtrC\ pGtrABC}$	SB300	*ΔoafA gtrC(a)::cat* pGtrABC	Sm, Cm, Amp	This work
S.Tm^{GFP}	SB300	Wild-Type strain SB300 pM965	Sm, Amp	This work
Evolved clones				
Evolved clone O:4,12	*S*.Tm$^{\Delta sseD}$	*sseD::aphT;* clone R423A	Sm, Kan	This work
Evolved clone 1 O:5,12^{Bimodal}	*S*.Tm$^{\Delta sseD}$	*sseD::aphT;* clone R421B	Sm, Kan	This work
Evolved clone 2 O:4,12^{Bimodal}	*S*.Tm$^{\Delta sseD}$	*sseD::aphT;* clone R423B	Sm, Kan	This work
Evolved clone 3 O:5,12^{Bimodal}	*S*.Tm$^{\Delta sseD}$	*sseD::aphT;* clone R430B	Sm, Kan	This work
Evoltrap evolved clones	*S*.Tm^{WT}		Sm	This work
Plasmids	**Backbone**	**Relevant genotype**	**Resistance***	**Reference**
pM965	pSC101	P_{rpsM}-*gfp*	Amp	***Stecher 2004*** (*44*)
pg*trABC*	pM965	P_{rpsM}-*gtrABC*(a)	Amp	This work
pKD46			Amp	***Datsenko 2000*** (*42*)
pCP20			Amp, Cm	***Datsenko 2000*** (*42*)
pKD3			Cm	***Datsenko 2000*** (*42*)
* Relevant resistances only: Sm = ≥50 µg/ml streptomycin; Cm = ≥6 µg/ml chloramphenicol; Kan = ≥50 µg/ml kanamycin; Amp = ≥100 µg/ml ampicillin.				

Supplementary Table 2: Primers used in this study

Primer name	Sequence	Purpose	Reference
oafA_Seq_up	CCGCCATAGTTACGTTTTG	Sequencing oafA	This work
oafA_Seq_dw	AAGCTATACACATAAAATAATTTGC		This work
oafA_IntSeq1_up	AGTACTTGATTTTTATATTGCAAG		This work
oafA_IntSeq2_up	GAGGTTTATGGGATAGTCC		This work
oafA_IntSeq3_up	GCCTGATATTTGCTTCCTC		This work
oafA_IntSeq4_up	CCGTAATCTGAGAGATAATGA		This work
Del_oafA_up	AATTATAGGTAAAAAATGATCTACAAGAAATTCAGACTCGTGTGTAGGCTGGAGCTGCTTC	In frame deletion *oafA*	This work
Del_oafA_dw	GGCAAGCCCCTCTGTTTATTTTGAAATCTGCTTTTTCACTCATATGAATATCCTCCTTAG		This work
Ver_oafA_up	ATGTAGTTGATGTAACAGGTC	Deletion verification *oafA*	This work
Ver_oafA_dw	ATGCCCCATCAGAAAAGCT		This work
Ver_STM0558_up	ATTGGTGTGATAAATCCTATTG	Deletion verification *gtrC*(a)	This work
Ver_STM0558_dw	GCTATCAGCCTGATATGCG		This work
Ver_STM4205_up	GTAATCATCAGAGTGAATAGG	Deletion verification *gtrC*(b)	This work
Ver_STM4205_dw	CGCAATTAGCCTTATTTGCG		This work
Del_wca_wza_up	TAAAAATAGCGGTACTTACCCTCCCCGCTTCGGCAGCGAATGTGTAGGCTGGAGCTGCTTC	Deletion cluster *wca-wza*	This work
Del_wca_wza_dw	AGTGATAAATAATCAATGATGAAATCCAAAATGAAATTGACATATGAATATCCTCCTTAG		This work
Ver_wca_wza_up	CCATAACATTAAGTATGAACAACT	Verification deletion cluster *wca-wza*	This work
Ver_wca_wza_dw	AAGCCGCTATTTAAATTGCACA		This work
Del_0712-23_up	TGATGGATTTGTTTTGTGAAAAGAAAATATCTTACGCAAGTGTGTAGGCTGGAGCTGCTTC	Deletion cluster SaltsV1_0712 to SaltsV1_0723	This work
Del_0712-23_dw	GGAATTAAATGACGCTTAGTTATATTTTGCCCAAAATTTTCATATGAATATCCTCCTTAG		This work
Ver_0712-23_up	ATTAAACTCATCTGATCAGTGAT	Verification deletion cluster SaltsV1_0712 to SaltsV1_0723	This work
Ver_0712-23_dw	GGCGAGCGCCCAATAAT		This work
Del_0559_up	CGACTAACGAGATTTTCATTTCGCATCCCTAAAGACAATGTGTGTAGGCTGGAGCTGCTTC	In frame deletion *gtrA(a)*	This work
Del_0559_dw	CCGCTGATTTTCATAATGTTGAAGTTATTCGCTAAGTACACATATGAATATCCTCCTTAG		This work
Ver_0559_up	TAGAAAATAGGTATCGTGGCT	Verification deletion *gtrA(a)*	This work
Ver_0559_dw	GTAGTGCTACACTCCAGAC		This work
Del_gtrC_up	ATAATTAAGAATGAGAAGAAAAATGGTTAACAATAGATTATGTGTAGGCTGGAGCTGCTTC	In frame deletion *gtrC(a)*	This work
Del_gtrC_dw	TACATGAATGTTATTTAATTATTTCCGTAATATTCTCATTCATATGAATATCCTCCTTAG		This work
Ver_gtrC_up	CGCCCGTTACCCATTGG	Verification deletion *gtrC(a)*	This work
Ver_gtrC_dw	TTGATAGGAATAGGTATTCTTGG		This work
Del_wzyB_up	TTCTAAAGGCTCTATATGCTTATAATTTCATACATTGCATTATGCTGTGCAGGCTGGAGCTGCTTC	In frame deletion *wzyB*	This work
Del_wzyB_dw	TTGCCGCCGTATAACTTATTTATTGTTTCTTAGTAAAACGAATCTCATATGAATATCCTCCTTAG		This work
Ver_wzyB_up	CCAACAAGCTTTACAGGAAC	Verification deletion *wzyB*	This work
Ver_wzyB_dw	GATTCAGAATATCTTGCCAGA		This work
PstI_Gtr57.59_up	ATCGTACTGCAGATGTTGAAGTTATTCGCTAAGTA	Cloning *gtrABC(a)*	This work
EcoRV_Gtr57.59_dw	GTAATCGATATCGGCGGGGAACATTAATTATAC		This work
SeqInt1_gtrABC	CATACATCCTCTATTACTCATC	Sequencing P*rpsM-gtrABC(a)*	This work
SeqInt2_gtrABC	ATCTCTTGTAGTTGTATTAATTTCT		This work
SeqInt3_gtrABC	TAATTAAGAATGAGAAGAAAAATGGT		This work
SeqInt4_gtrABC	GGTGCTGGCTAAGCGC		This work
SeqInt5_gtrABC	CAGCTGTCTTACGCTTCAT		This work
SeqInt6_gtrABC	ATCAGCCTGATATGCGGATT		This work

Supplementary Table 3: Mutations detected in genome sequencing of O:12^{Bimodal} clones
Numbers in parentheses indicate the number of reads covering the indicated position in the genome.

	Ancestor	Evolved (Chronic infection, day 36)							
Clone name	**Ancestor M556**	R423A	R421B	R423B	R430B				
Staining with O:5 antisera	Positive	Negative	Positive	Negative	Positive				
Staining with O:12 antibody	Positive	Positive	Bimodal	Bimodal	Bimodal				
Serotype	**O5:12**	**O:4,12**	**O:5,12 [12-2]**	**O:4,12 [12-2]**	**O:5,12 [12-2]**				
						Reference	Allele	Region	Function
					13832..13843 (43)	GGCGGCGGATTT	-	*dnaJ*	Chaperone protein DnaJ
	635606 (98)	635606 (97)	635606 (99)	635606 (100)	635606 (100)	T	A	STM0576	putative PTS system mannose-specific enzyme IIAB
	1756092 (100)	1756092 (98)	1756092 (100)	1756092 (95)	1756092 (98)	G	A	*yciT*	putative regulatory protein
		2330274..2330280 (100)		2330274..2330280 (76)		ATTTTAT	-	*oafA*	O antigen acetylase
				2388693..2388694 (100)		TG	C		
				2388696 (100)		C	A	Deletion *glpA*	sn-glycerol-3-phosphate dehydrogenase subunit A
				2388699 (100)		A	T		
	2411272 (100)	2411272 (99)	2411272 (99)	2411272 (100)	2411272 (100)	T	C	*menC*	o-succinylbenzoate synthase
	2433677 (100)	2433677 (99)	2433677 (100)	2433677 (100)	2433677 (100)	T	G	*nuoF*	NADH-quinone oxidoreductase subunit F
		2728584..2728589 (64)				GCAAGG	-	intergenic	Prophage Gifsy-1
					3035159 (100)	C	T	*hilC*	Transcriptional regulator HilC
					4810867 (98)	A	G	*tsr*	methyl-accepting chemotaxis protein I
		4810885 (98)		4810885 (98)		G	A		
			4905774 (22)			T	G	*creD*	conserved exported protein of unknown function